Rivelatori per astronomia X e gamma dallo spazio parte 2

A. Bulgarelli, V. Fioretti

(INAF/IASF Bologna)

Andrea Bulgarelli (bulgarelli@iasfbo.inaf.it)
Valentina Fioretti (fioretti@iasfbo.inaf.it)

Table of Contents

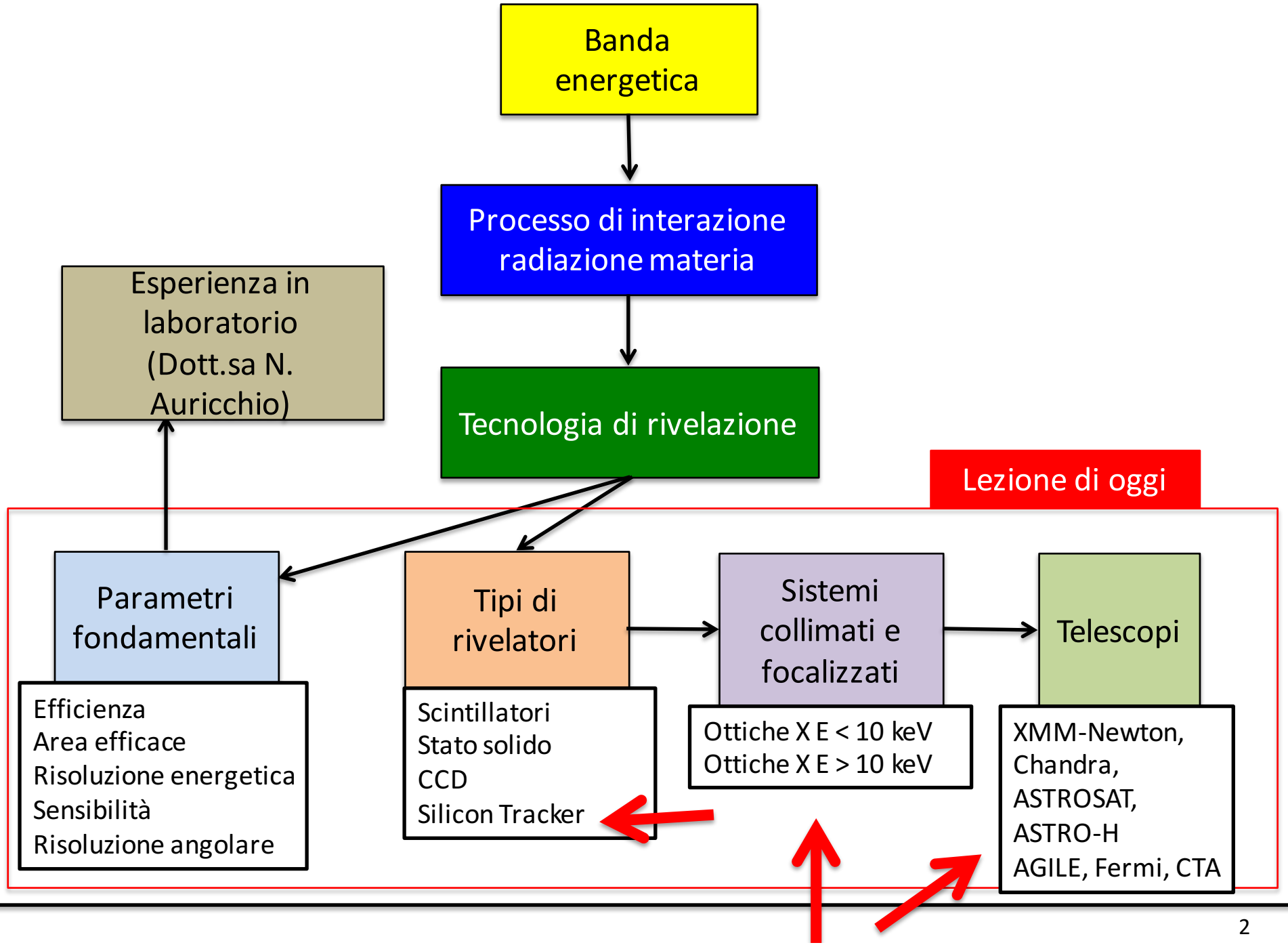

Gamma-Ray Detectors (pair production)

Andrea Bulgarelli (bulgarelli@iasfbo.inaf.it)

Silicon Trackers

Astronomia gamma dallo spazio

- The main purpose of a Silicon Tracker is to provide a compact **imager** for gamma-ray photons of energy **above 10 MeV**.
- The Tracker plays two roles at the same time:
  - it **converts the gamma-rays** in heavy-Z material layers (245 um of Tungsten), where the photon interacts producing an electron/positron pair in the detector,
  - and **records the electron/positron** tracks by a sophisticated combination of Silicon microstrip detectors and associated readout.

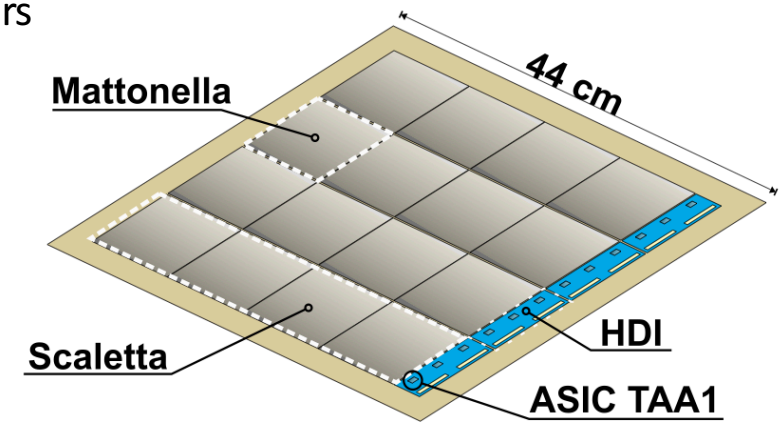

Figura 3.2: Vista di un piano assemblato del tracciatore: sono evidenziati, sopra lo strato di kapton, le singole mattonelle di silicio e le scalette, di fronte alle quali si notano gli ASIC di lettura posti sull'HDI.

12 piani

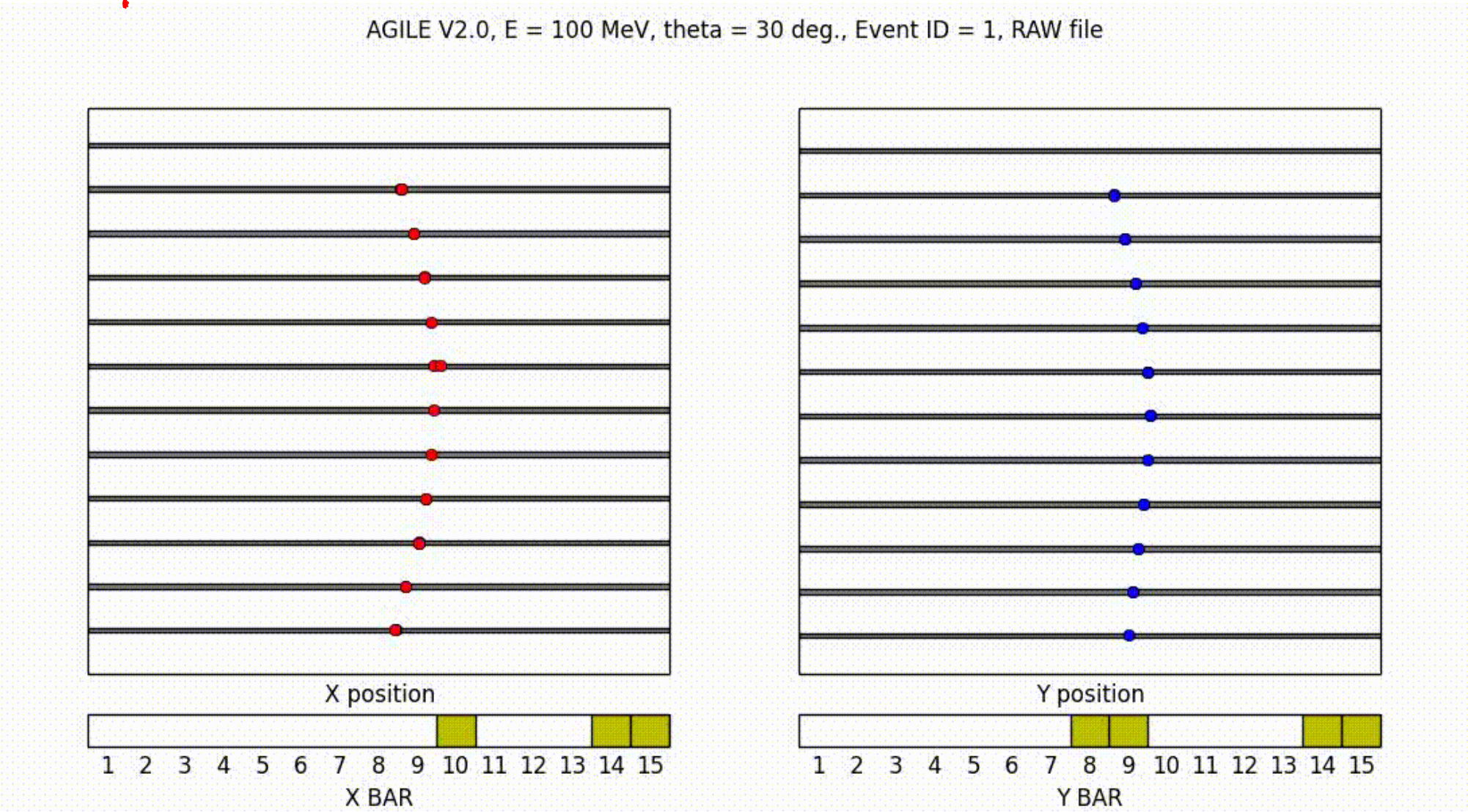
AGILE V2.0, E = 100 MeV, theta = 30 deg., Event ID = 1, RAW file
X position
1 2 3 4 5 6 7 8 9 10 11 12 13 14 15
X BAR
Y position
1 2 3 4 5 6 7 8 9 10 11 12 13 14 15
Y BAR

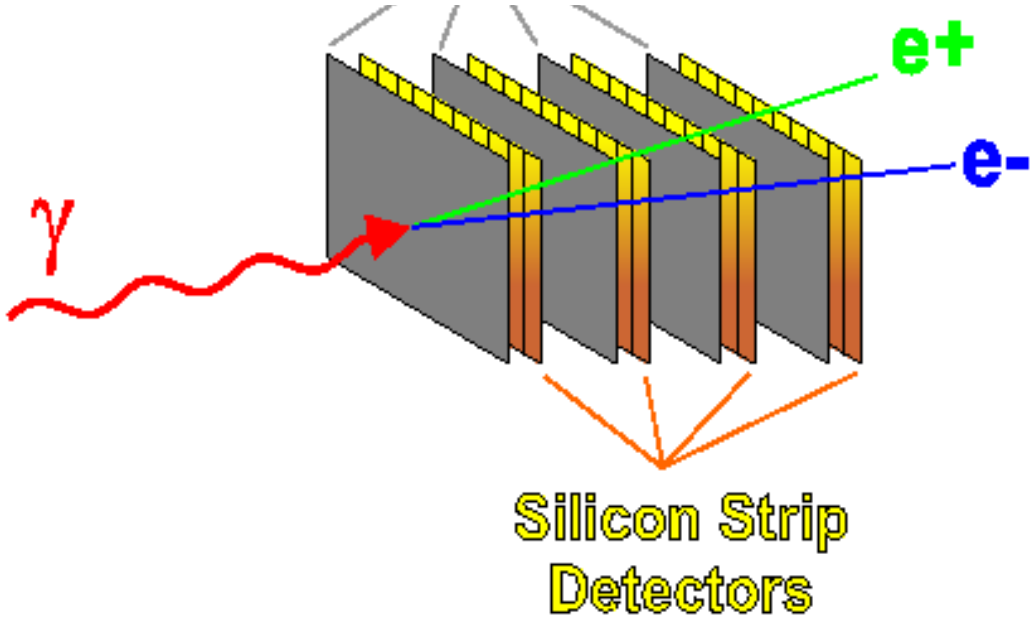

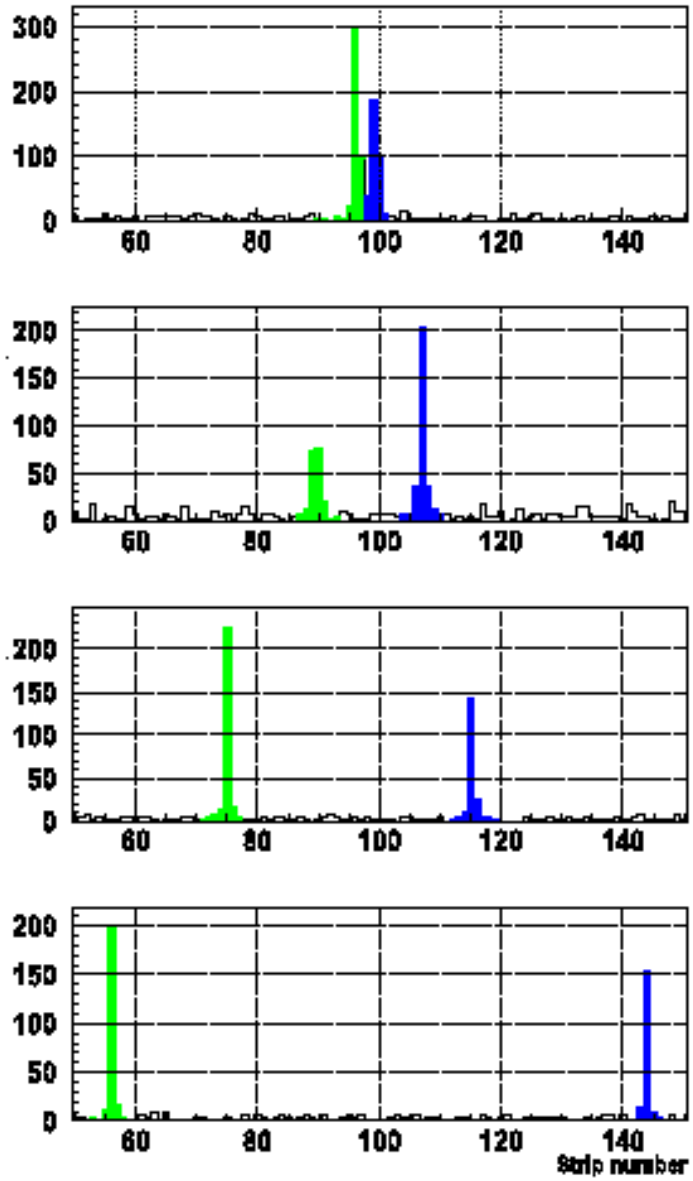

An event is a collection of all the electron/positron interactions into the microstrips of the silicon detector (each interaction generates a cluster that is a group of neighboring strips collecting the charge deposited by the particle)

A complete representation of the event topology allows the reconstruction of the incoming direction and energy of the gamma-ray.

PHOTAG TESTBEAM - INFN TS/IFC MI

Rivelazione indiretta dei gamma: che cosa complica la ricostruzione?

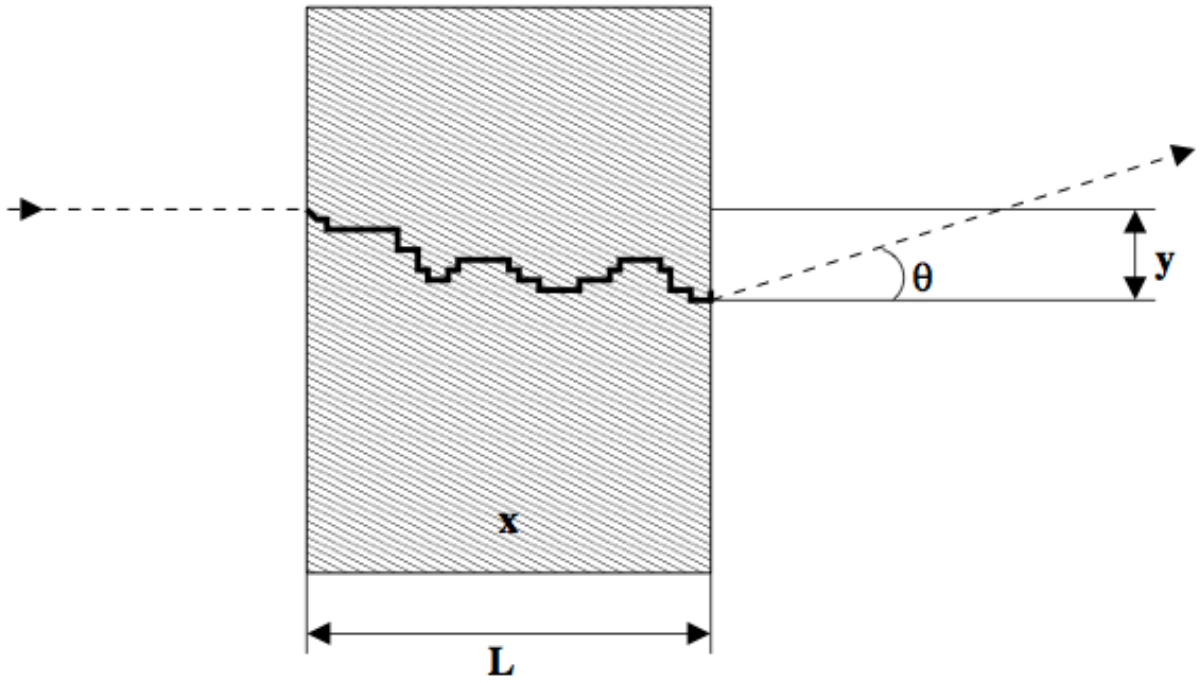

Figura 3.9: Multiplo scattering: spostamento dalla traiettoria (y) di una particella c
atttaversa uno spessore di x lunghezze di radiazione e lunghezza L.

L'elettrone e il positrone, interagendo con la materia presente lungo il loro cammino, sono soggetti a variazione di traiettoria dovuta allo **scattering multiplo di tipo coloumbiano**. Questo effetto ha luogo soprattutto nel tungsteno, che se da un lato è necessario per la conversione, dall'altro causa una perdita progressiva dell'informazione sulla direzione del fotone incidente.

The AGILE Silicon Tracker (INFN-Ts)

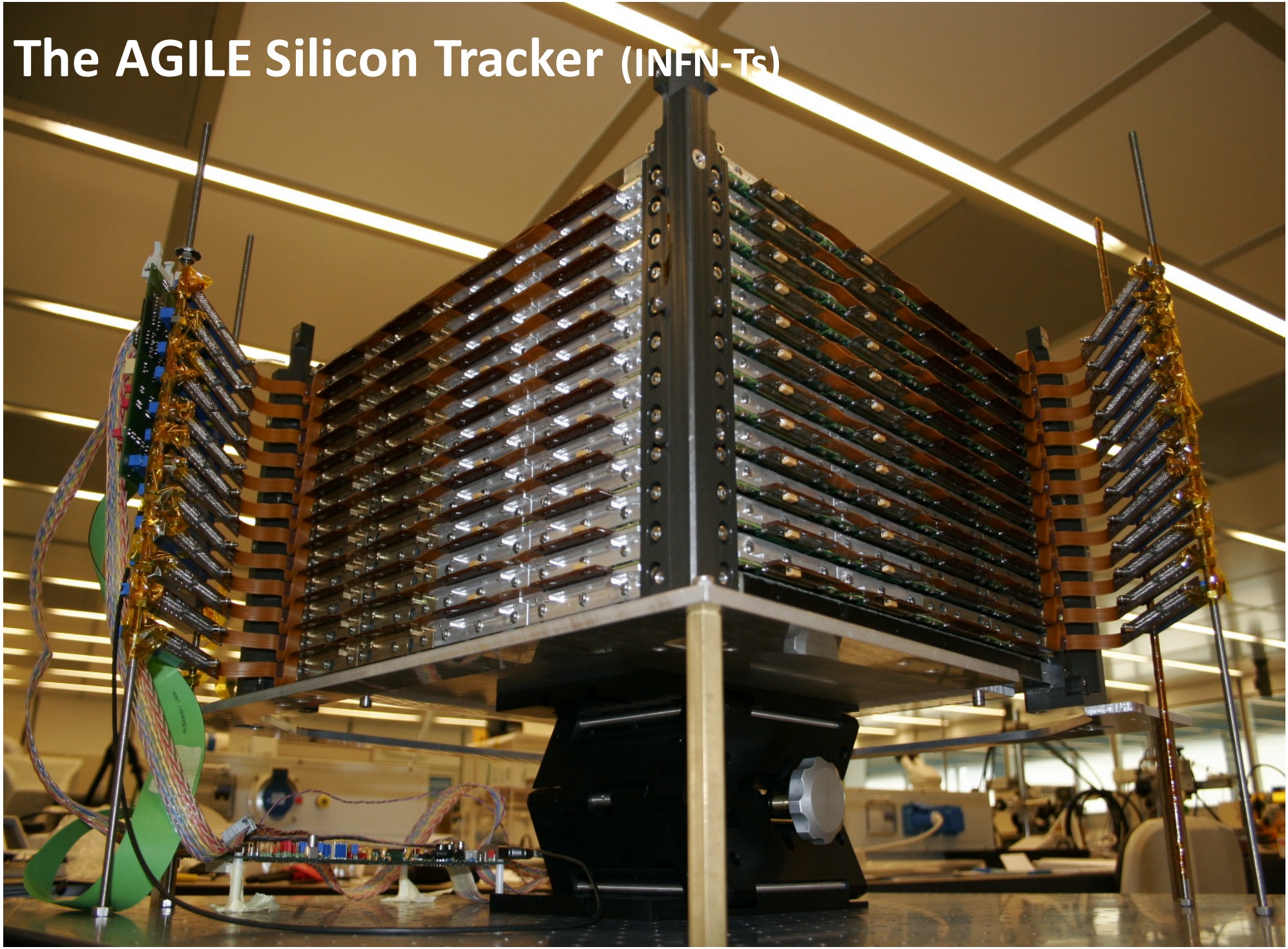

ASTROGAM (proposal): 70 piani, no W

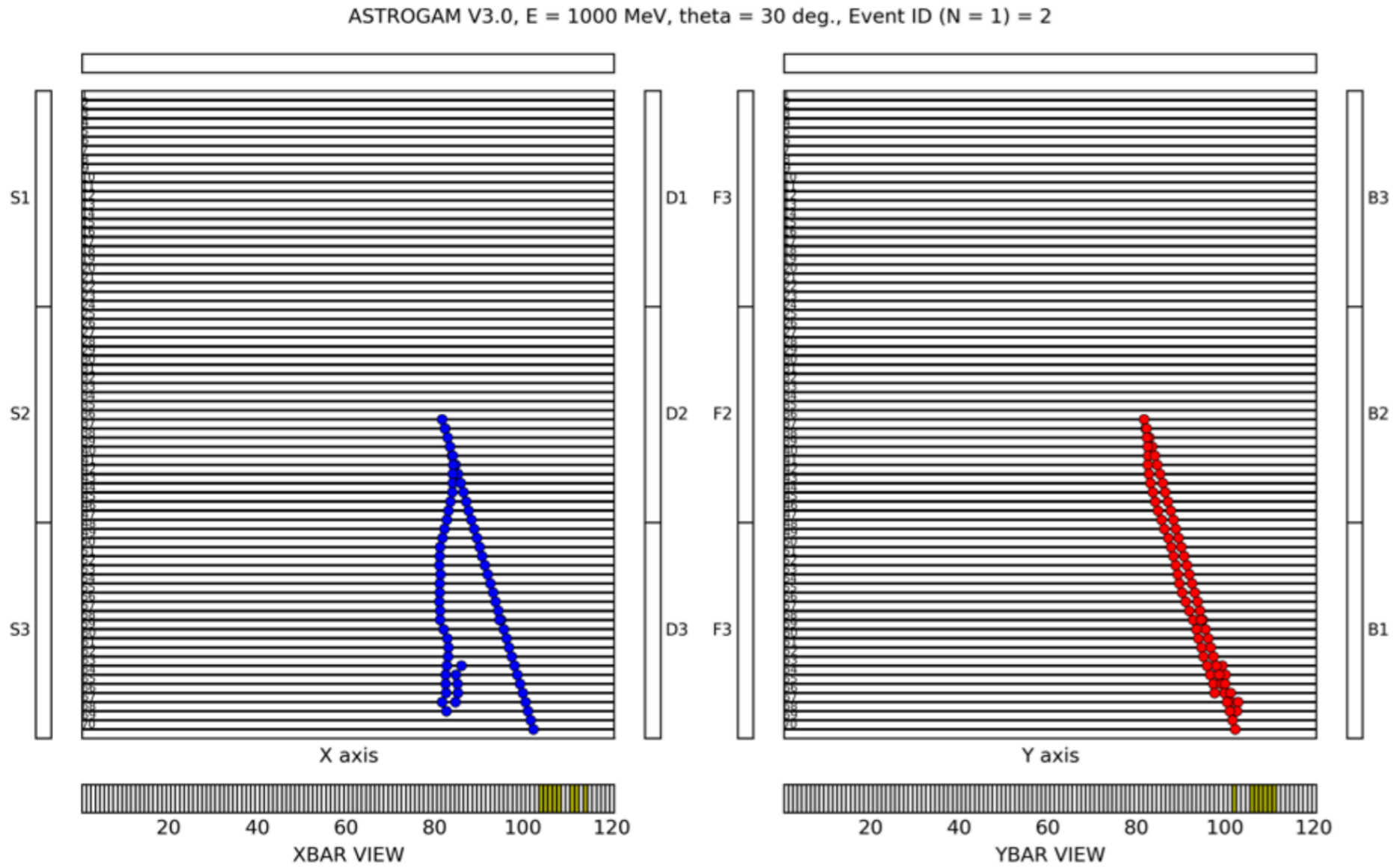

Ottiche X

Andrea Bulgarelli (bulgarelli@iasfbo.inaf.it)

limitare il segnale di background proveniente da zone lontane dall'oggetto osservato

Collimatori vs concentratori

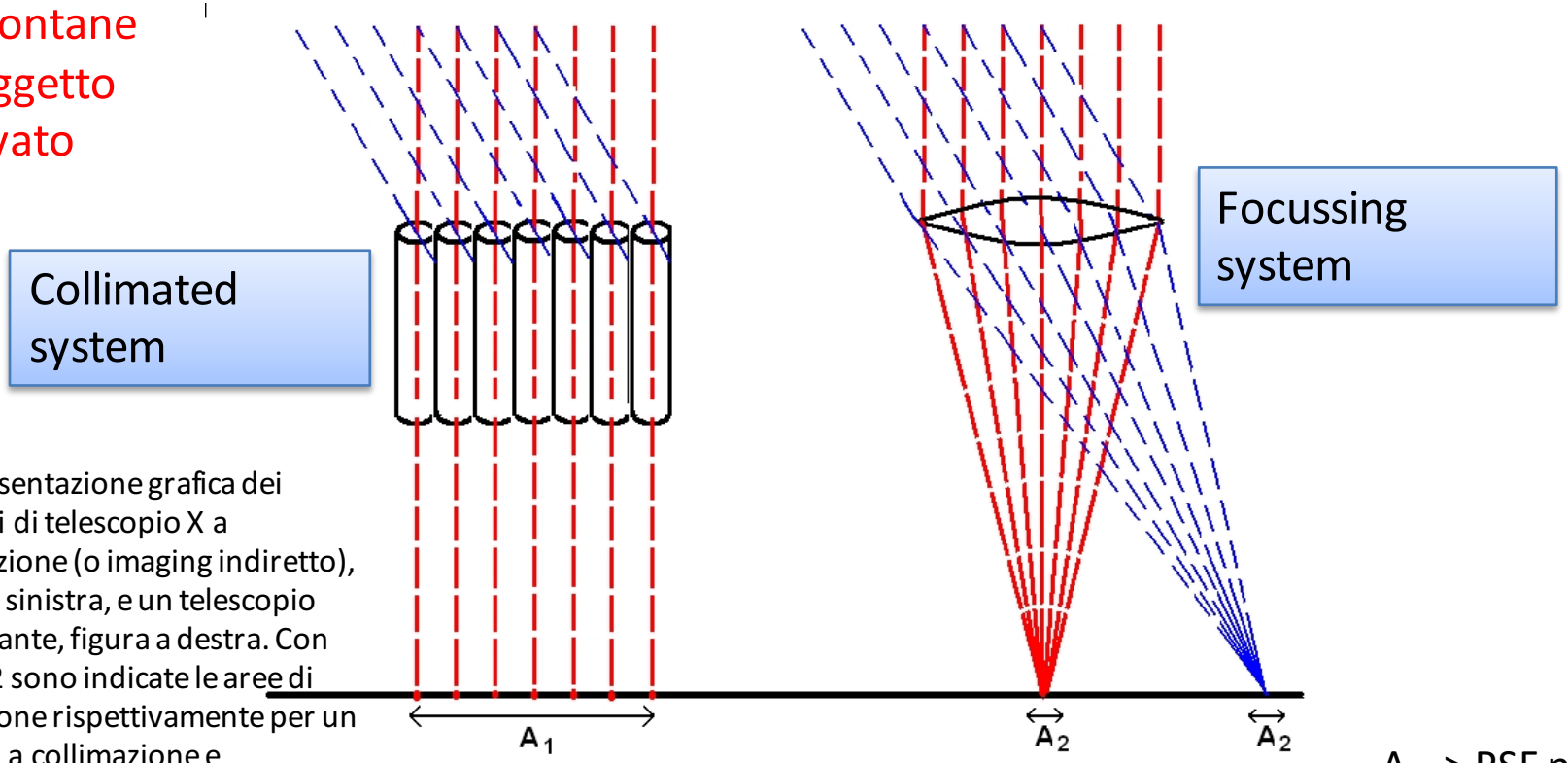

Rappresentazione grafica dei concetti di telescopio X a collimazione (o imaging indiretto), figura a sinistra, e un telescopio focalizzante, figura a destra. Con A1 e A2 sono indicate le aree di rivelazione rispettivamente per un sistema a collimazione e focalizzante. Si noti come nel secondo caso **l'area del rivelatore si riduce notevolmente**, il che si traduce in una corrispondente **diminuzione del fondo.**

$$\mathbf{F_{Min} = \frac{n_\sigma}{\varepsilon}\sqrt{\frac{B}{ATE}}}$$

$$F_{\min} = n_\sigma \frac{\sqrt{BA_d}}{A_{eff}\sqrt{T_{\text{int}}\,\Delta E}}$$

A_d -> PSF proiettata sul piano focale (in cm^2).
F_{min} -> A_{eff}^{-1} -> aumentare la sensibilità senza aumentare le dimensioni

il sistema focalizzato in figura (rappresentato con una lente), concentra il segnale di un fattore A1/A2, permettendo così di rilevare segnali molto deboli.

Ottiche X - Materiali

- Missioni attuali: fino a 10 keV, pianificato fino a 80 keV
- **difficoltà** principale nella costruzione di ottiche per raggi X = tutti i materiali hanno nei raggi X un indice di rifrazione n appena inferiore a 1 ed un alto coefficiente di assorbimento. Ciò **esclude** la possibilità di sfruttare la **rifrazione per realizzare lenti**;
- è possibile invece produrre ottiche a **riflessione** grazie al fenomeno della **riflessione totale dei raggi X in incidenza radente**: applicando la legge di Snell della rifrazione, **se l'angolo tra fascio e superficie diviene inferiore all'angolo critico** $\theta c = \arccos(n)$ (n = indice di rifrazione del materiale di coating) per la riflessione totale, **il fascio viene totalmente riflesso dallo strato**. In milliradianti

$$\theta_c \approx 28\,(\rho\, Z / A)^{1/2}\, E^{-1}$$

- esso **cresce** perciò **con la densità ρ** (espressa in g/cm3) del materiale usato per lo strato riflettente e **decresce con l'energia E** (espressa in keV) dei fotoni, oltre a dipendere dal rapporto Z (numero atomico)/ A (peso atomico) dell'elemento
- Facilitare la riflessione totale = riflettere ad angoli meno radenti
  - vengono quindi **usati materiali ad alta densità**, come Oro, *Platino, Iridio, per i quali l'angolo critico è più grande (ed è di alcuni gradi per fotoni di 1 keV).*

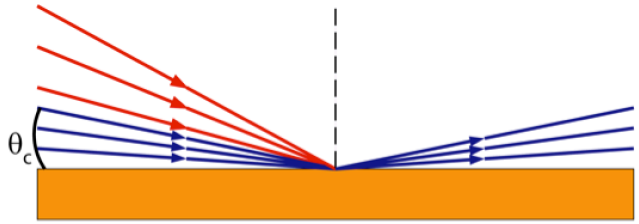

X-ray reflection

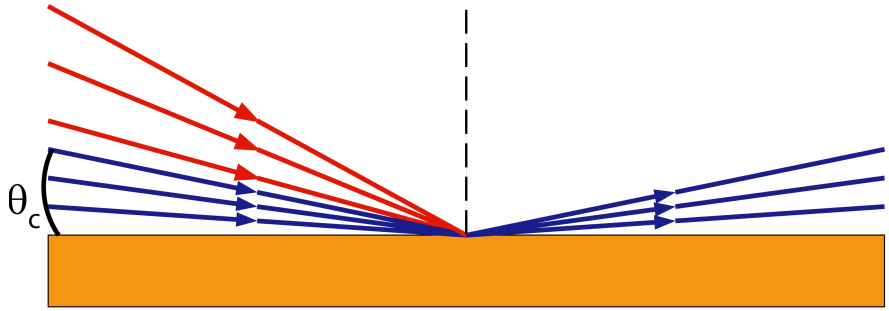

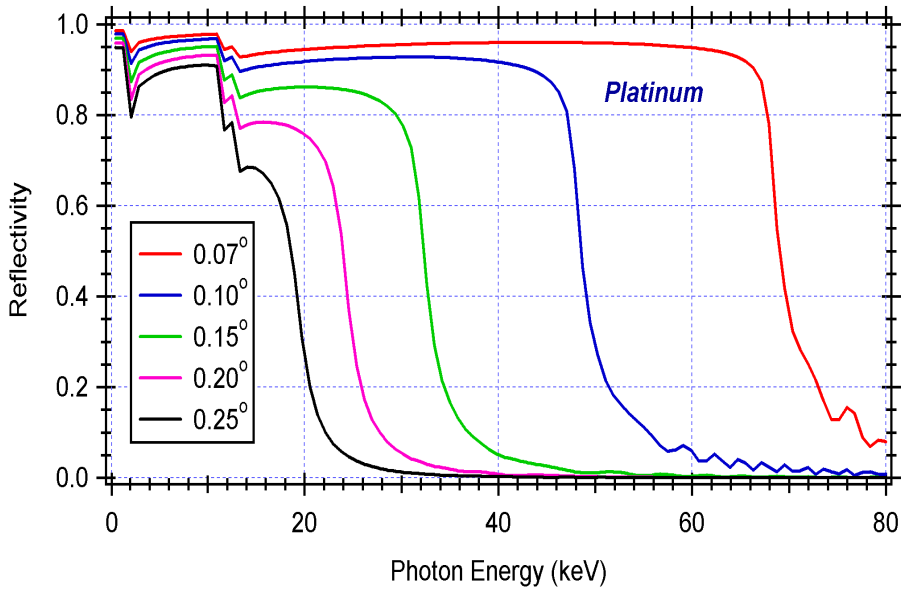

$$\vartheta_{crit} \propto \frac{\sqrt{\rho}}{E}$$

- High Z materials (Au, Pt, Ir)
- critical angle (few degrees for E = 1 keV)

Per una fissata energia, quindi, i fotoni incidenti sullo strato sarebbero teoricamente riflessi al 100% (in realtà, parte dei fotoni vengono assorbiti dalla superficie **e la riflettività è sempre leggermente inferiore a 1**).
Similmente, **per un angolo di incidenza fissato**, è immediato verificare che esiste **un'energia critica** al di sotto della quale la riflettività è poco inferiore a 1; superato l'angolo critico e l'energia critica, la riflettività decade rapidamente a zero.

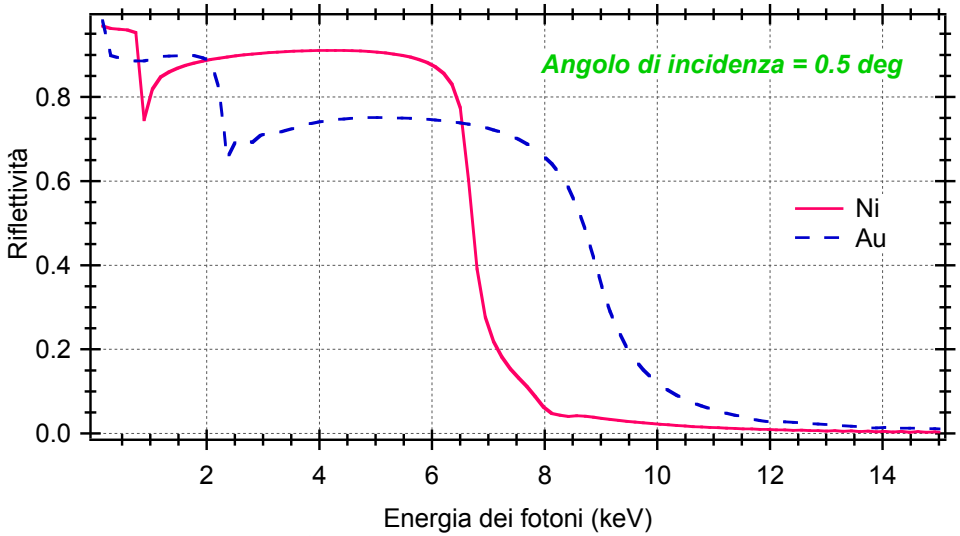

Wolter 1 profile for X-ray astronomy

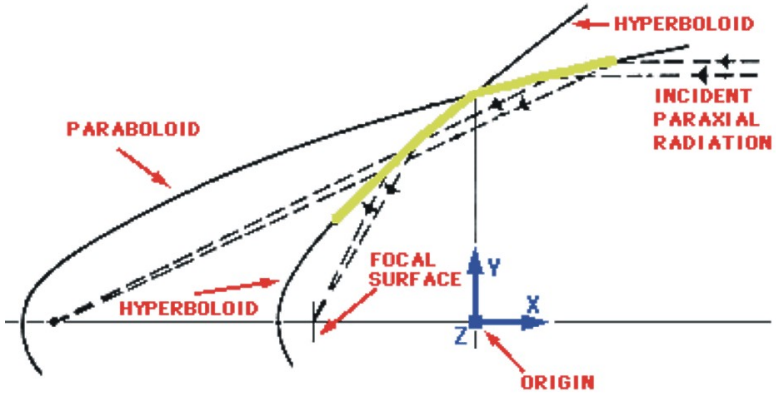

F = focal length **R = reflectivity**

L = mirror height **θ = incidence angle**

$$Aeff \approx F^2 \times \theta_c^2 \times R^2$$

L'incidenza radente vincola la geometria dello specchio: un profilo usato per **minimizzare** le aberrazioni di coma ed aumentare il campo di vista del telescopio sfrutta una doppia riflessione su un paraboloide e su un iperboloide di rivoluzione

Con questo profilo si minimizza la lunghezza focale F

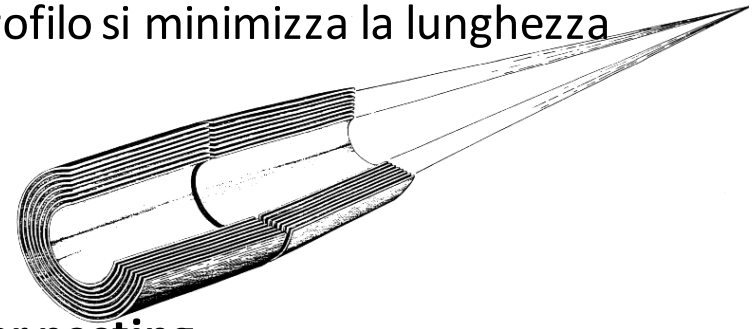

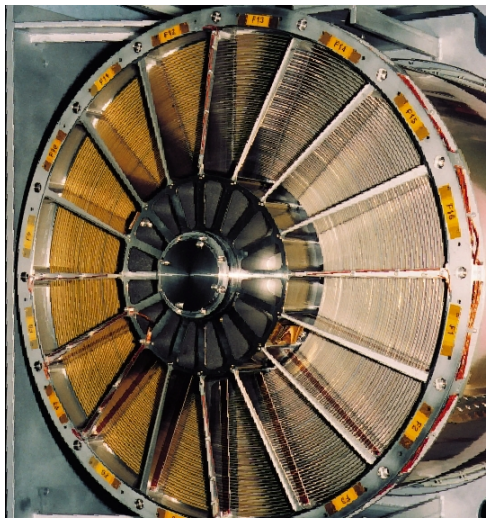

Co-focal mirror nesting

Sistemi di specchi di questo tipo, confocali e di diametro decrescente, vengono innestati uno dentro l'altro. Per nidificare molti specchi -> molto sottili (0.5 – 1 mm), ma sufficientemente rigidi da conservare il profilo corretto. Problema della massa

X-ray focussing at E > 10 keV

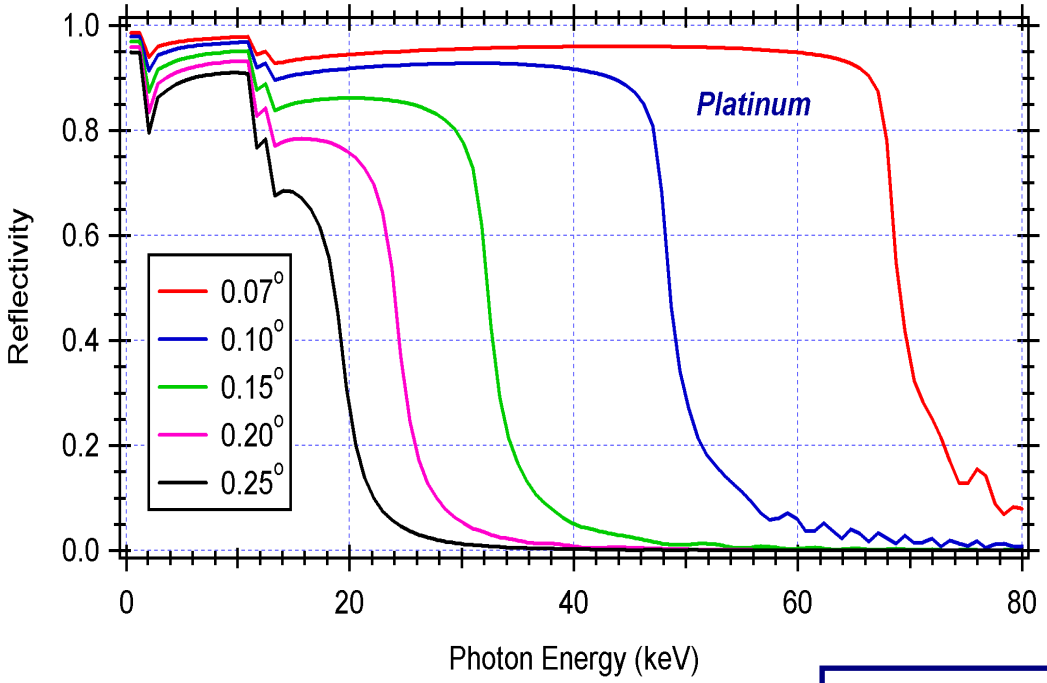

but

$$\vartheta_{crit} \propto \frac{\sqrt{\rho}}{E}$$

At photon energies > 10 keV the cut-off angles for total reflection are very small also for heavy metals

the attained geometrical areas are in general negligible

Possible solutions…

$$Aeff \approx F^2 \times \theta_c^2 \times R^2$$

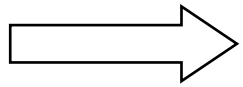

- large number of modules operating in parallel
- large focal lengths (10 - 100 m)
- use of very high density single-layer reflecting coatings (Ir o Pt)
- use of supermirror multilayer coatings →

Multi-layers for hard X-ray astronomy

- Anche utilizzando materiali ad alta densità, poco oltre i 10 keV l'angolo critico per l'incidenza radente diventa troppo piccolo (< 0.25°) da rendere insufficiente l'area utile di raccolta dell'ottica, a meno di ricorrere a focali superiori ai 10 m, difficili da utilizzare su telescopi costituiti da un singolo satellite.
- Multilayer coating → tecnica utilizzabile per riflettere raggi X oltre i 10 keV ad angoli di incidenza di 0.2° – 0.4°
- **strati alternati (bistrati)** di un materiale ad **alta densità** (ad esempio Platino o Tungsteno) e di uno **a bassa densità** (Silicio o Carbonio); lo spessore degli strati è dell'ordine di qualche nanometro
- Riflettività ottenuta per ***interferenza costruttiva***

Multi-layers for hard X-ray astronomy (>10 keV)

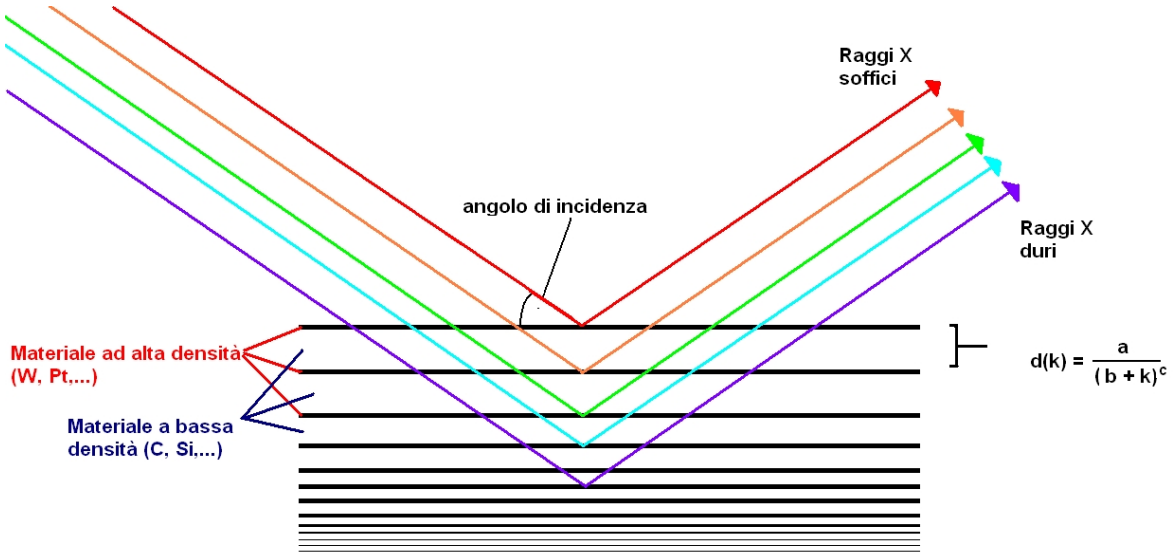

*Multilayer coatings allow high reflectance beyond the critical angle by **constructive interference** of rays reflected at properly spaced Pt/C or W/Si bi-layers (200 bilayers, 60A*200=1micron).*

If the d-spacing is changed in continuous way along the sequence, and the photoelectric absorption is not too large, it is possible to get reflection windows 3-4 times larger than in total reflection regime.

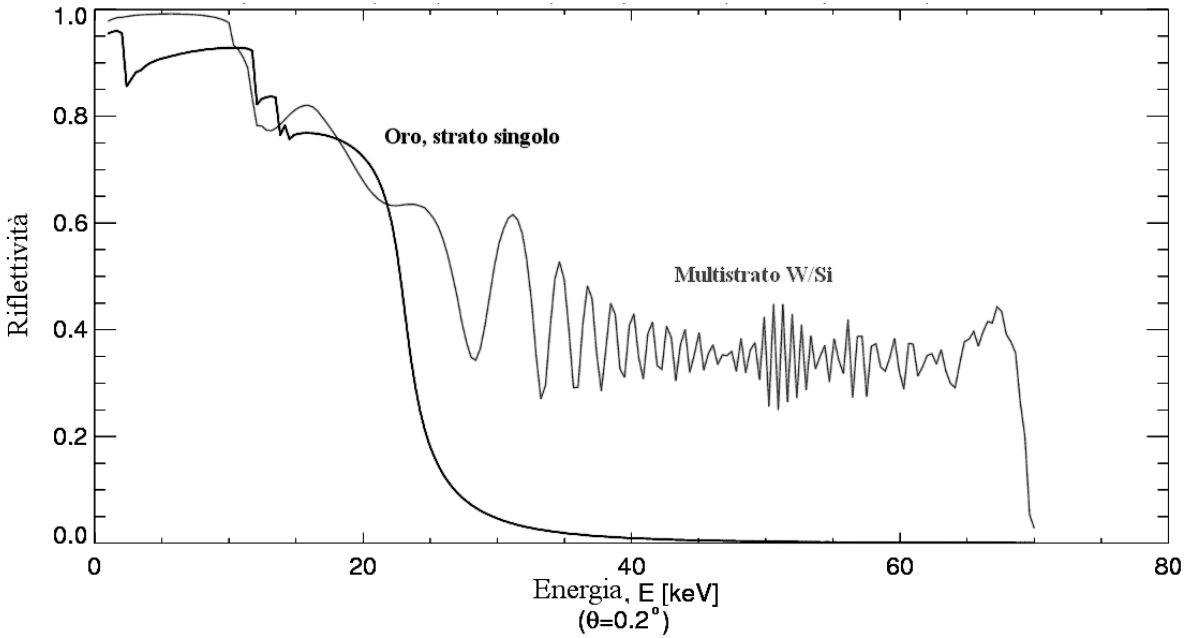

The optimal distribution of layer spacing follows in general a power law (a,b,c are parameters that should be optimezed):

$d(i) = a / (b+i)^c$

i = bilayer index

$a \approx \lambda/(2 \sin \theta_{inc})$ $c \approx 0.25$ $b > -1$

Orbite

Andrea Bulgarelli (bulgarelli@iasfbo.inaf.it)

Altitude classification: LEO, MEO, HEO

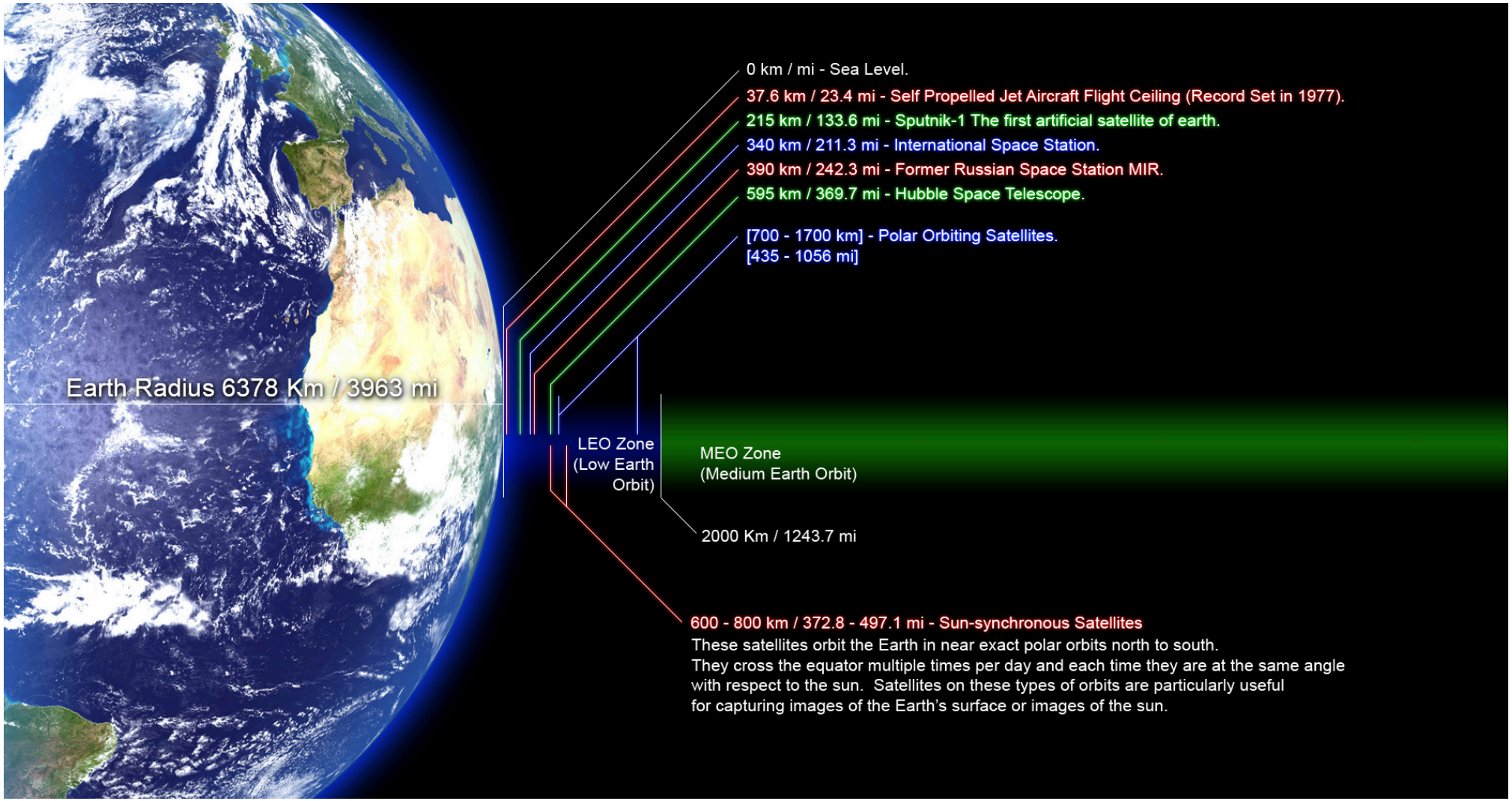

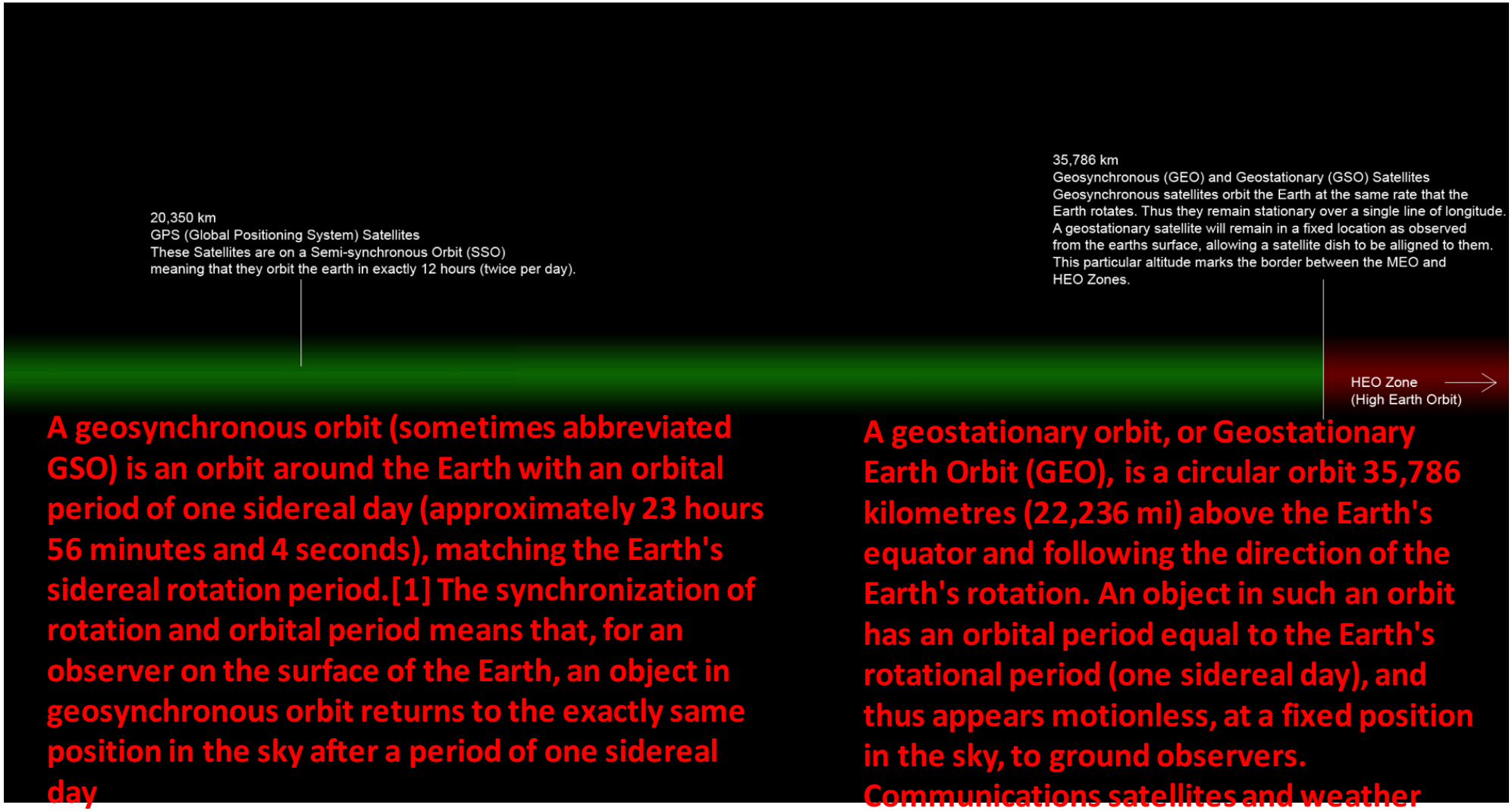

A geosynchronous orbit (sometimes abbreviated GSO) is an orbit around the Earth with an orbital period of one sidereal day (approximately 23 hours 56 minutes and 4 seconds), matching the Earth's sidereal rotation period.[1] The synchronization of rotation and orbital period means that, for an observer on the surface of the Earth, an object in geosynchronous orbit returns to the exactly same position in the sky after a period of one sidereal day

A geostationary orbit, or Geostationary Earth Orbit (GEO), is a circular orbit 35,786 kilometres (22,236 mi) above the Earth's equator and following the direction of the Earth's rotation. An object in such an orbit has an orbital period equal to the Earth's rotational period (one sidereal day), and thus appears motionless, at a fixed position in the sky, to ground observers. Communications satellites and weather satellites are often given geostationary orbits

LEO

- Objects in LEO encounter **atmospheric drag** in the form of gases in the thermosphere (approximately 80–500 km up) or exosphere (approximately 500 km and up), depending on orbit height.
- LEO is an orbit around Earth between the atmosphere and **below the inner Van Allen radiation belt**. The altitude is usually not less than 300 km because that would be impractical due to the larger atmospheric drag.
- **Equatorial low Earth orbits (ELEO)** are a subset of LEO. These orbits, with low inclination to the Equator, allow rapid revisit times and have the lowest delta-v requirement of any orbit. Orbits with a high inclination angle are usually called **polar orbits**.

Eccentricity classifications

- **Circular orbit**: An orbit that has an eccentricity of 0 and whose path traces a circle.
- **Elliptic orbit**: An orbit with an eccentricity greater than 0 and less than 1 whose orbit traces the path of an ellipse.
  - Geosynchronous transfer orbit: An elliptic orbit where the perigee is at the altitude of a Low Earth orbit (LEO) and the apogee at the altitude of a geosynchronous orbit.
  - Geostationary transfer orbit: An elliptic orbit where the perigee is at the altitude of a Low Earth orbit (LEO) and the apogee at the altitude of a geostationary orbit.
  - Molniya orbit: A highly elliptic orbit with inclination of 63.4° and orbital period of half of a sidereal day (roughly 12 hours). Such a satellite spends most of its time over two designated areas of the planet (specifically Russia and the United States).
  - Tundra orbit: A highly elliptic orbit with inclination of 63.4° and orbital period of one sidereal day (roughly 24 hours). Such a satellite spends most of its time over a single designated area of the planet.

XMM-Newton orbit

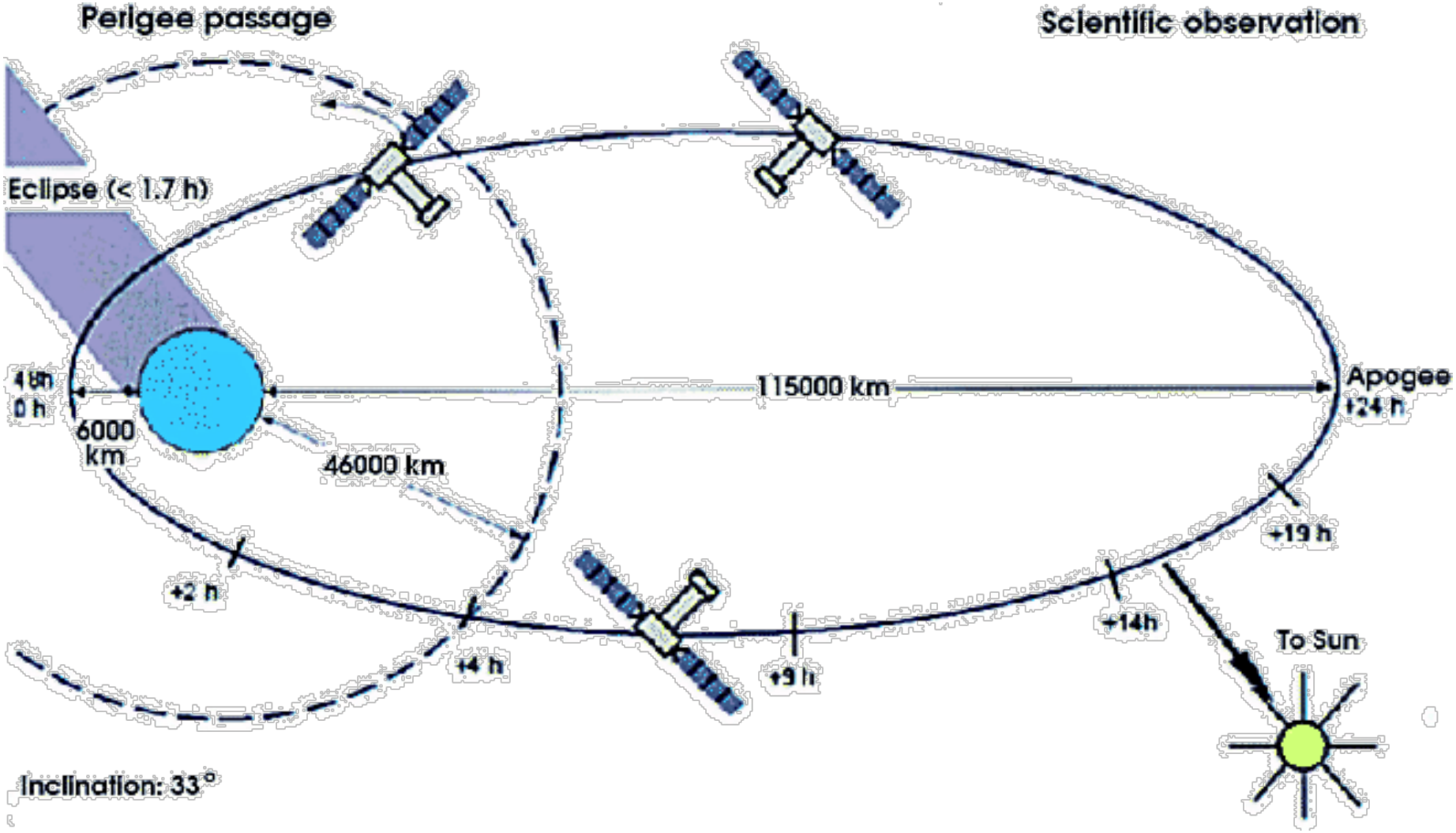

highly elliptical orbit, with an apogee of about 115,000 km and a perigee of ca. 6000 km
XMM is operated with three ground stations, located at Perth, Kourou and Santiago

Chandra orbit

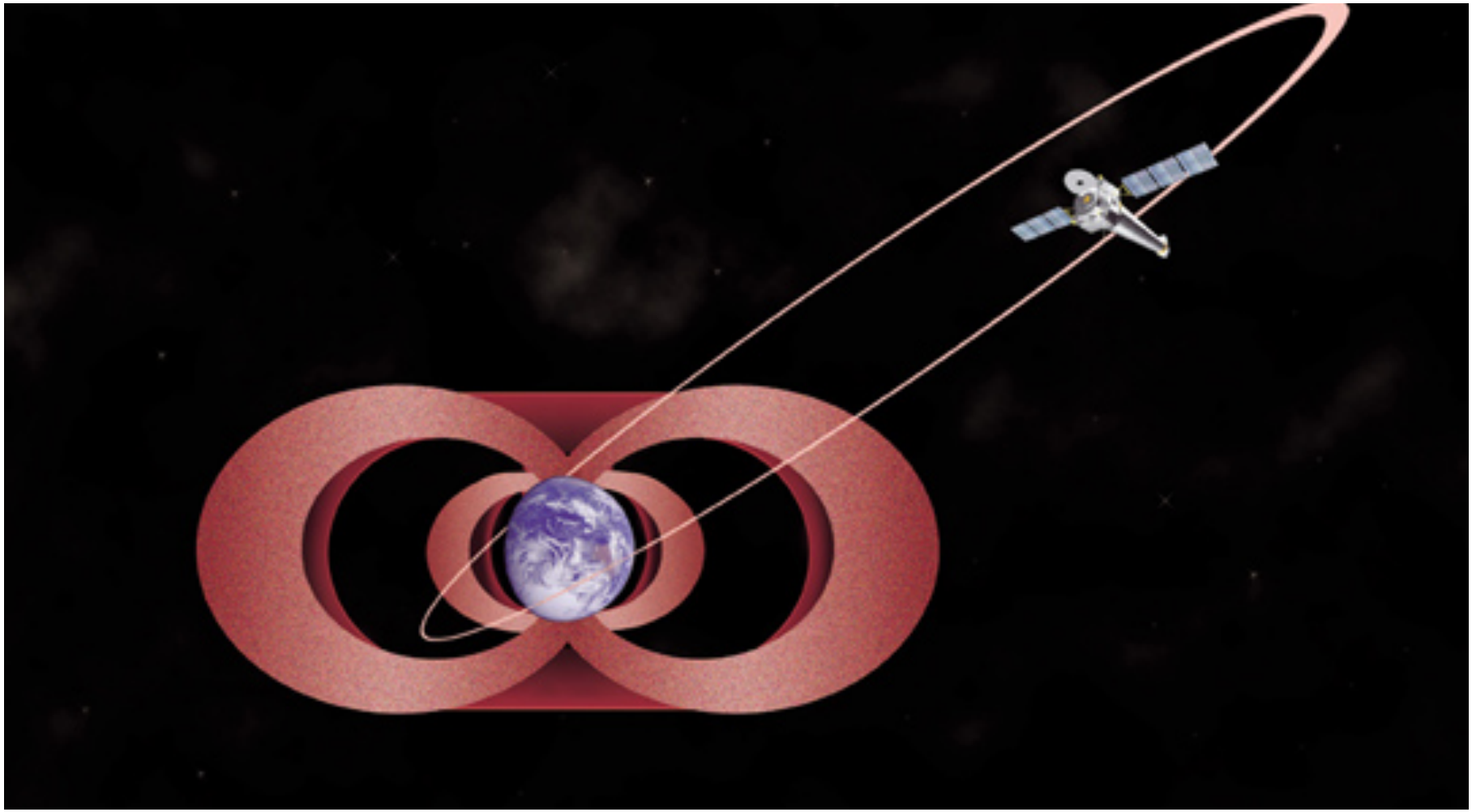

This elliptical orbit takes the spacecraft to an altitude of 133,000 km (82,646 mi) - more than a third of the distance to the moon - before returning to its closest approach to the Earth of 16,000 kilometers (9,942 mi). It takes approximately 64 hours and 18 minutes to complete an orbit.

L2 orbit

- the Lagrangian points are positions in an orbital configuration of two large bodies where a small object affected only by gravity can maintain a stable position relative to the two large bodies.
- Although the L1, L2, and L3 points are nominally unstable, it turns out that it is possible to find (unstable) periodic orbits around these points, at least in the restricted three-body problem.
- Sun–Earth L2

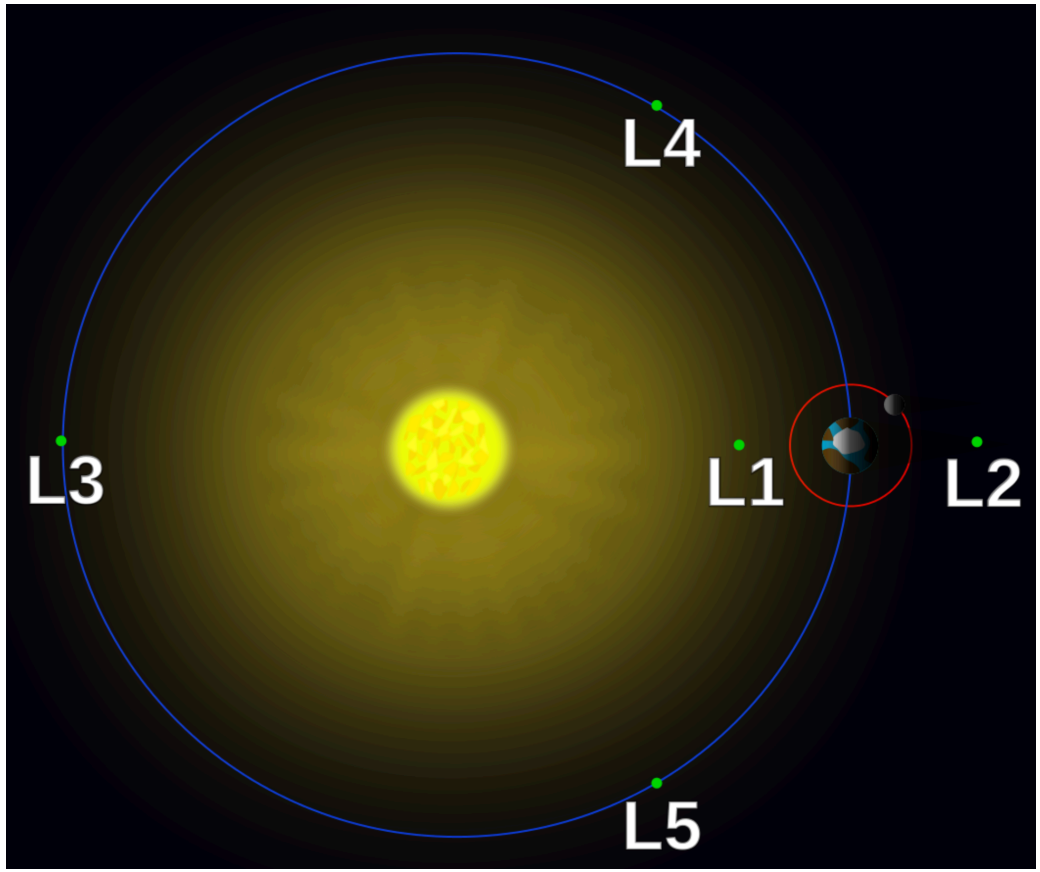

Missioni X e gamma presenti e future

Andrea Bulgarelli (bulgarelli@iasfbo.inaf.it)

Present and future X-ray and Gamma-ray missions

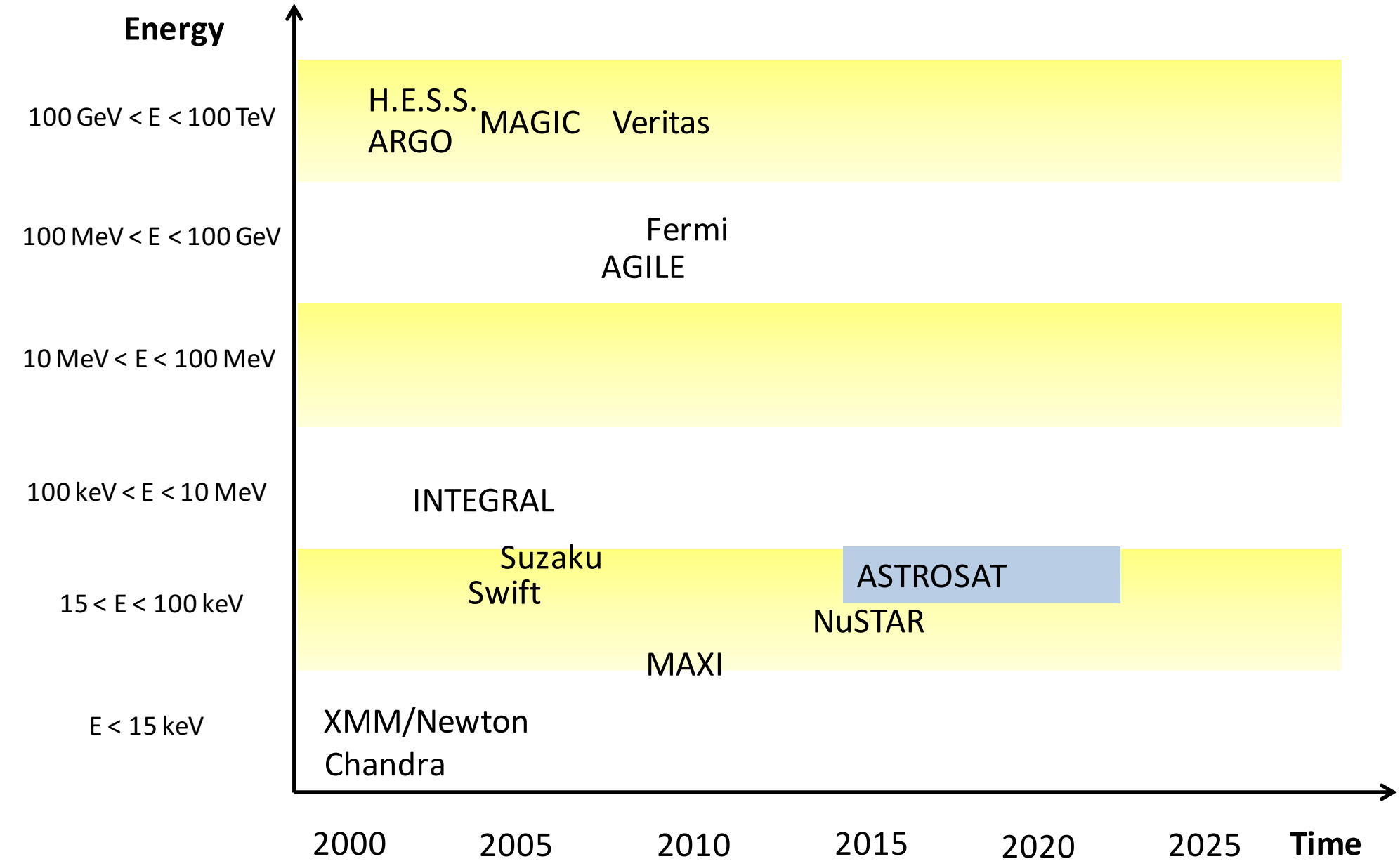

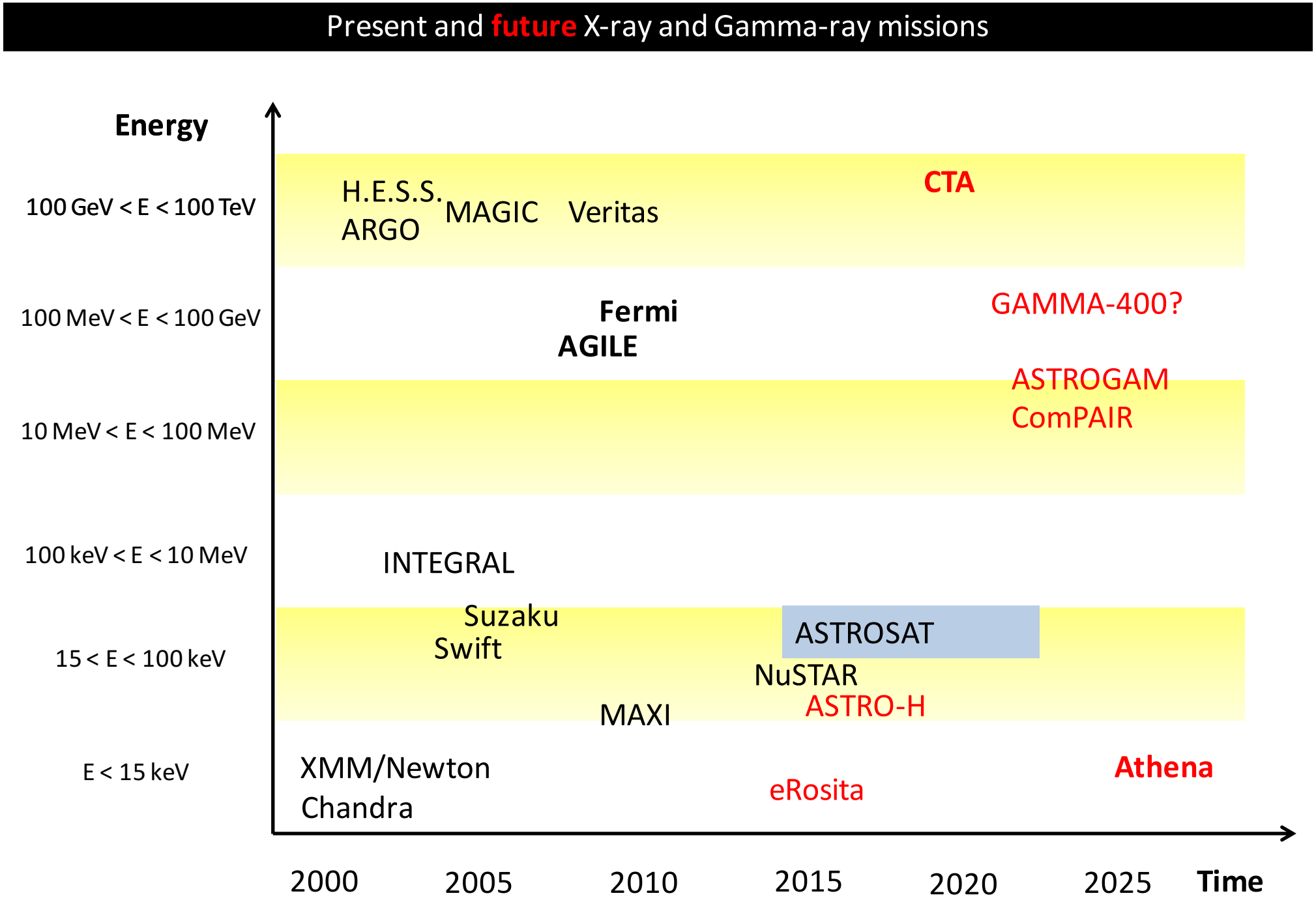
Present and future X-ray and Gamma-ray missions
Energy
100 GeV < E < 100 TeV
100 MeV < E < 100 GeV
10 MeV < E < 100 MeV
100 keV < E < 10 MeV
15 < E < 100 keV
E < 15 keV
H.E.S.S.
ARGO
MAGIC
Veritas
CTA
Fermi
AGILE
GAMMA-400?
ASTROGAM
ComPAIR
INTEGRAL
Suzaku
Swift
ASTROSAT
NuSTAR
MAXI
ASTRO-H
XMM/Newton
Chandra
eRosita
Athena
2000
2005
2010
2015
2020
2025
Time

ASTROSAT

A Soft X-ray Telescope (SXT) with conical foil mirrors and X-ray CCD detector, covering the energy range 0.3-8 keV.
The effective area will be about 120 sq.cm. at 1 keV.
LEO orbit (650 km)

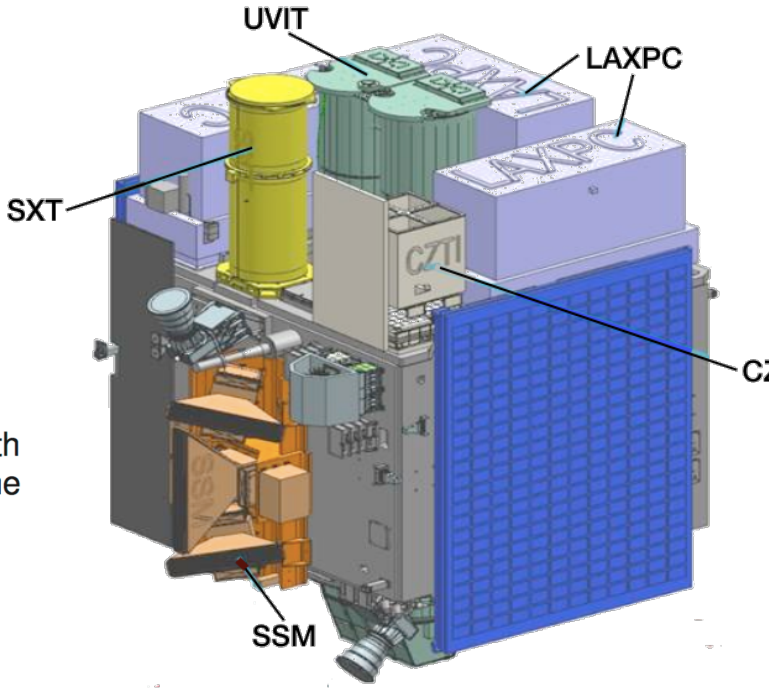

The Soft X-ray grazing incidence doubly reflecting Telescope (shown below with optics and camera) with a cooled CCD at its focus was launched on board the ASTROSAT on September 28th, 2015.

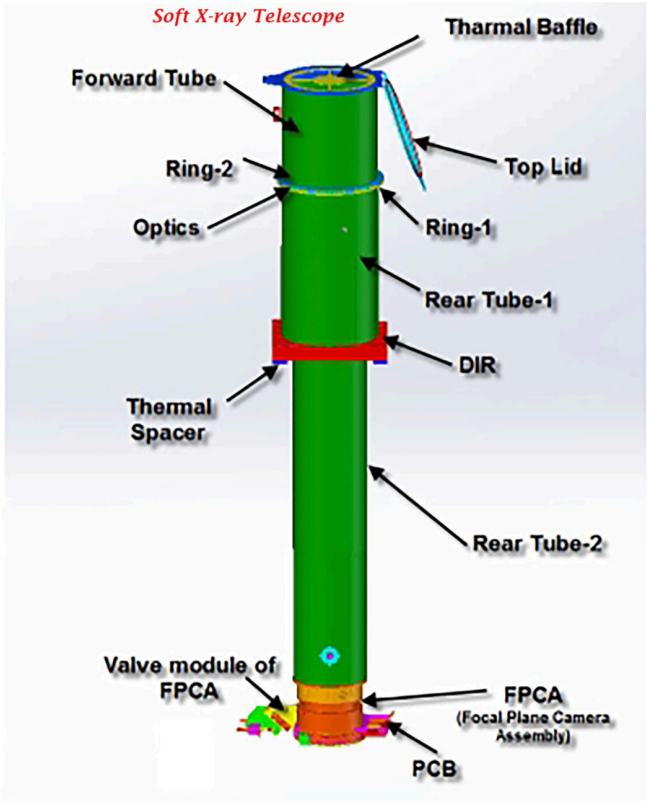

Schematic view of SXT

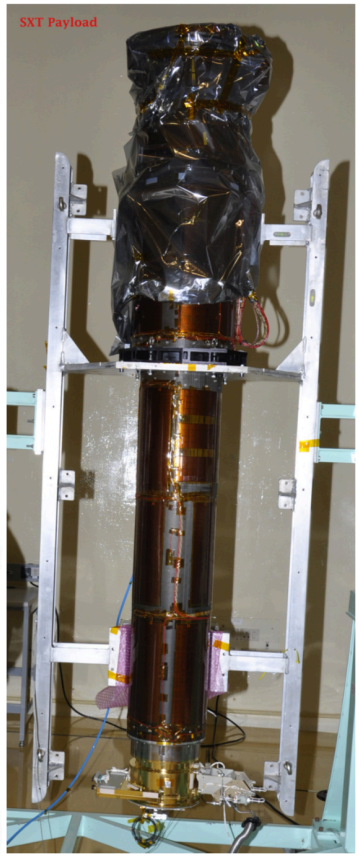

Actual view of SXT

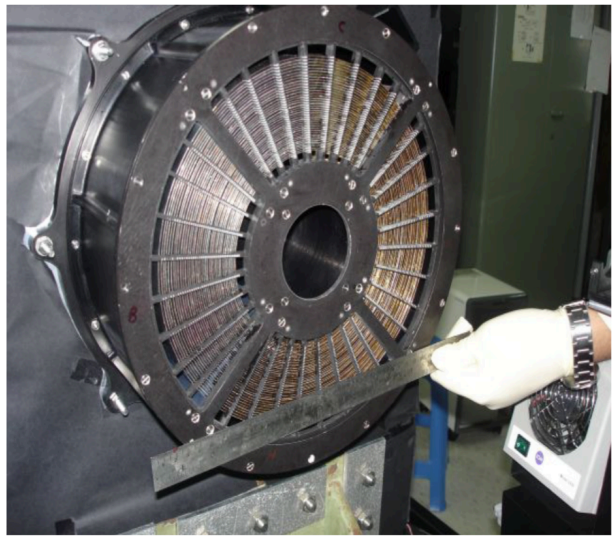

Front view of the assembled X-ray optics

ESA/ATHENA

ASI/
AGILE

NASA/Fermi

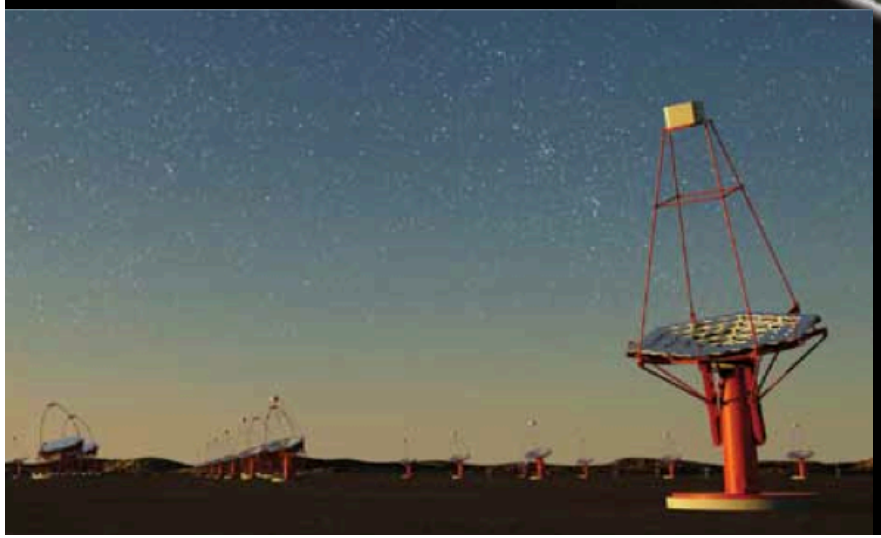

CTA

ATHENA

Andrea Bulgarelli (bulgarelli@iasfbo.inaf.it)

The Athena Observatory

Willingale et al, 2013
arXiv1308.6785

L2 orbit Ariane V
Mass < 5100 kg
Power 2500 W
5 year mission

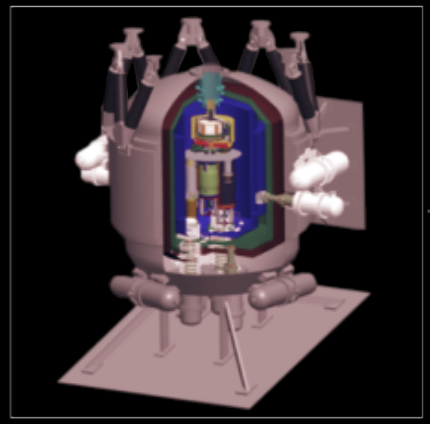

X-ray Integral Field Unit:
ΔE: 2.5 eV
Field of View: 5 arcmin
Operating temp: 50 mk

Barret et al., 2013 arXiv:1308.6784

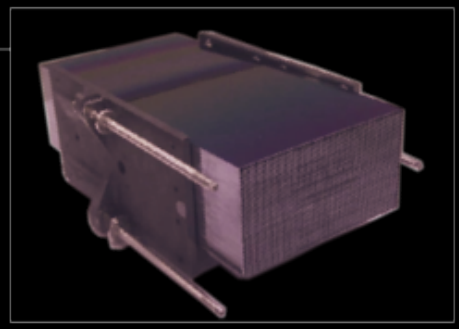

Silicon Pore Optics:
2 m^2 at 1 keV
5 arcsec HEW
Focal length: 12 m
Sensitivity: 3 10^{-17} erg cm^{-2} s^{-1}

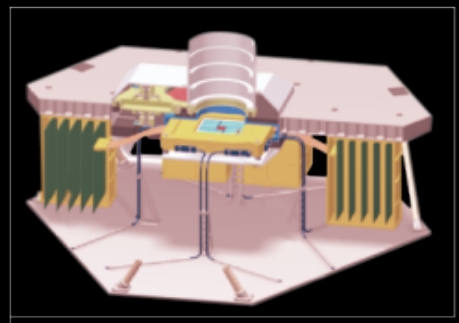

Wide Field Imager:
ΔE: 125 eV
Field of View: 40 arcmin
High countrate capability

Rau et al. 2013 arXiv1307.1709

The first Deep Universe X-ray Observatory

- Athena+ has vastly improved capabilities compared to current or planned facilities, and will provide **transformational** science on virtually all areas of astrophysics

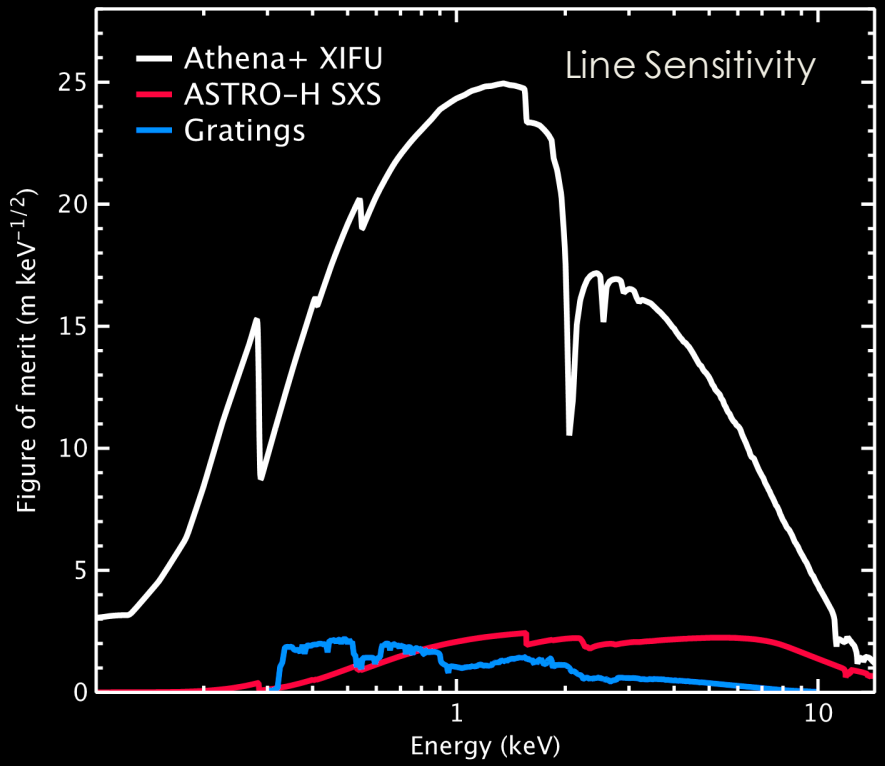

X-ray spectroscopy at the peak of the activity of the Universe

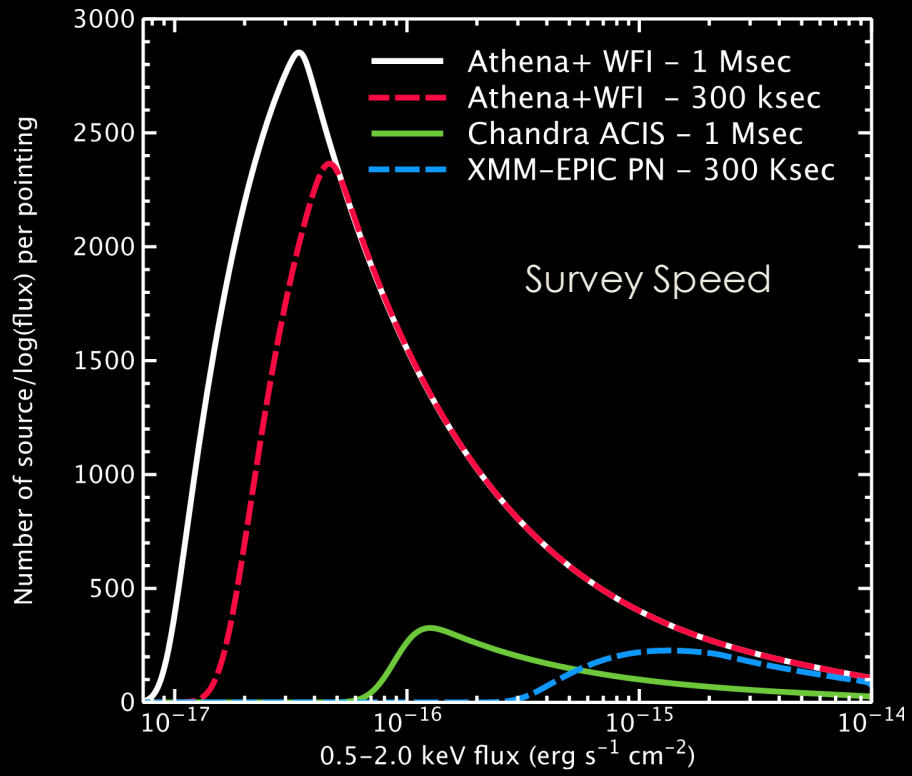

Deep survey capability into the dark ages and epoch of reionization

Athena science in context

Athena+ is a crucial part of the suite of large observatories needed to reach the science objectives of astronomy in the coming decades

AGILE

Andrea Bulgarelli (bulgarelli@iasfbo.inaf.it)

AGILE

KEY FEATURES

- **Italian gamma-ray telescope**
- **Similar to the Fermi Large Area Telescope, but about 1/16 the size**
- **FoV: 2.4 sr; 20% of the sky at any instant**
- **Launched April 23, 2007, from ISRO facility in Sriharikota, India**
- **Indian PSLV rocket**
- **AGILE is a gamma-ray observatory that work in the energy range 100 MeV – 50 GeV**
- **LEO orbit**
- PSF at 30◦ off-axis for E>100MeV of 2.1◦, for E>400 MeV of 1.1◦, and for *E>1 GeV of 0.8*◦

330 kg satellite

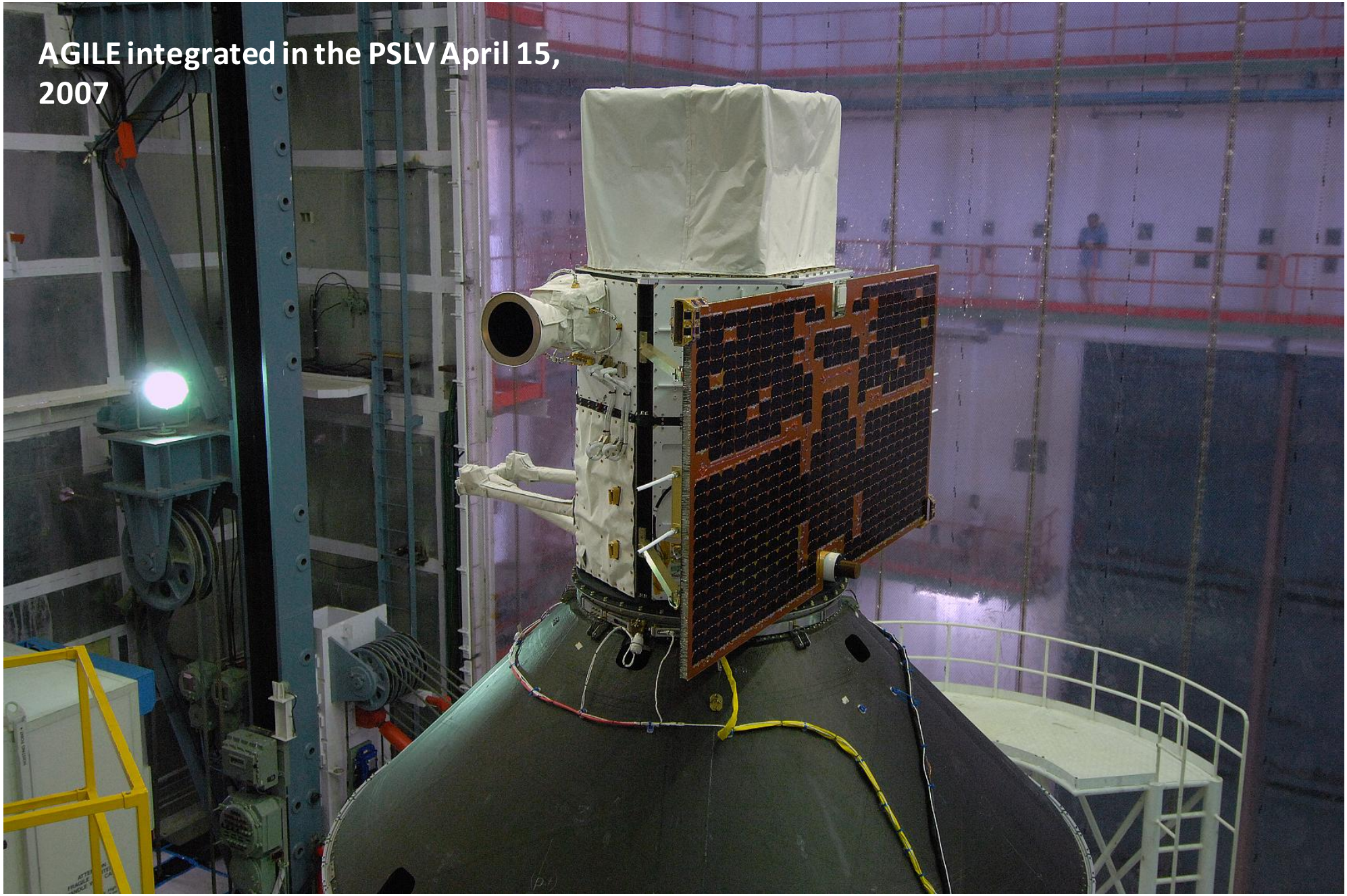

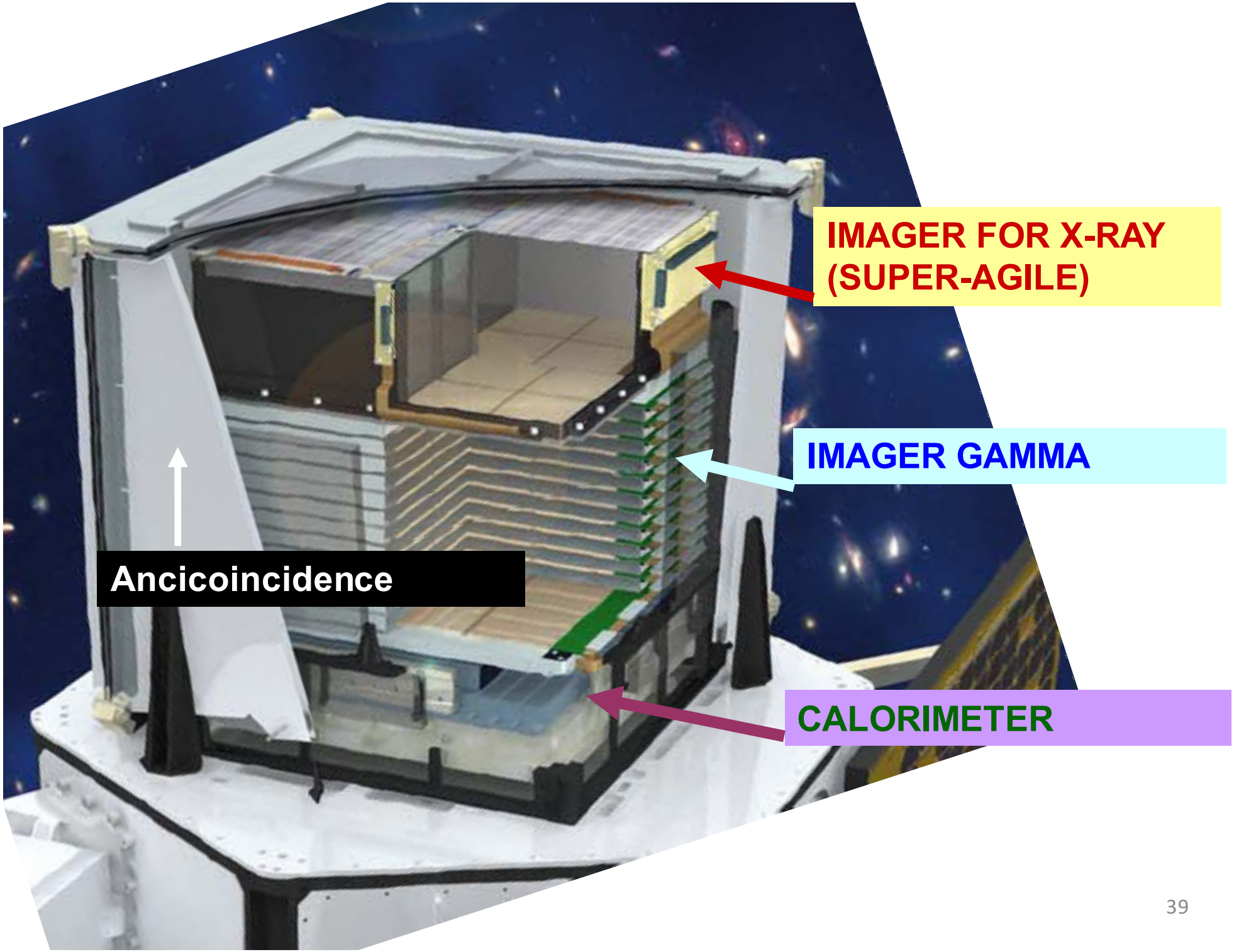
IMAGER FOR X-RAY
(SUPER-AGILE)
IMAGER GAMMA
Ancicoincidence
CALORIMETER

Large FoV?

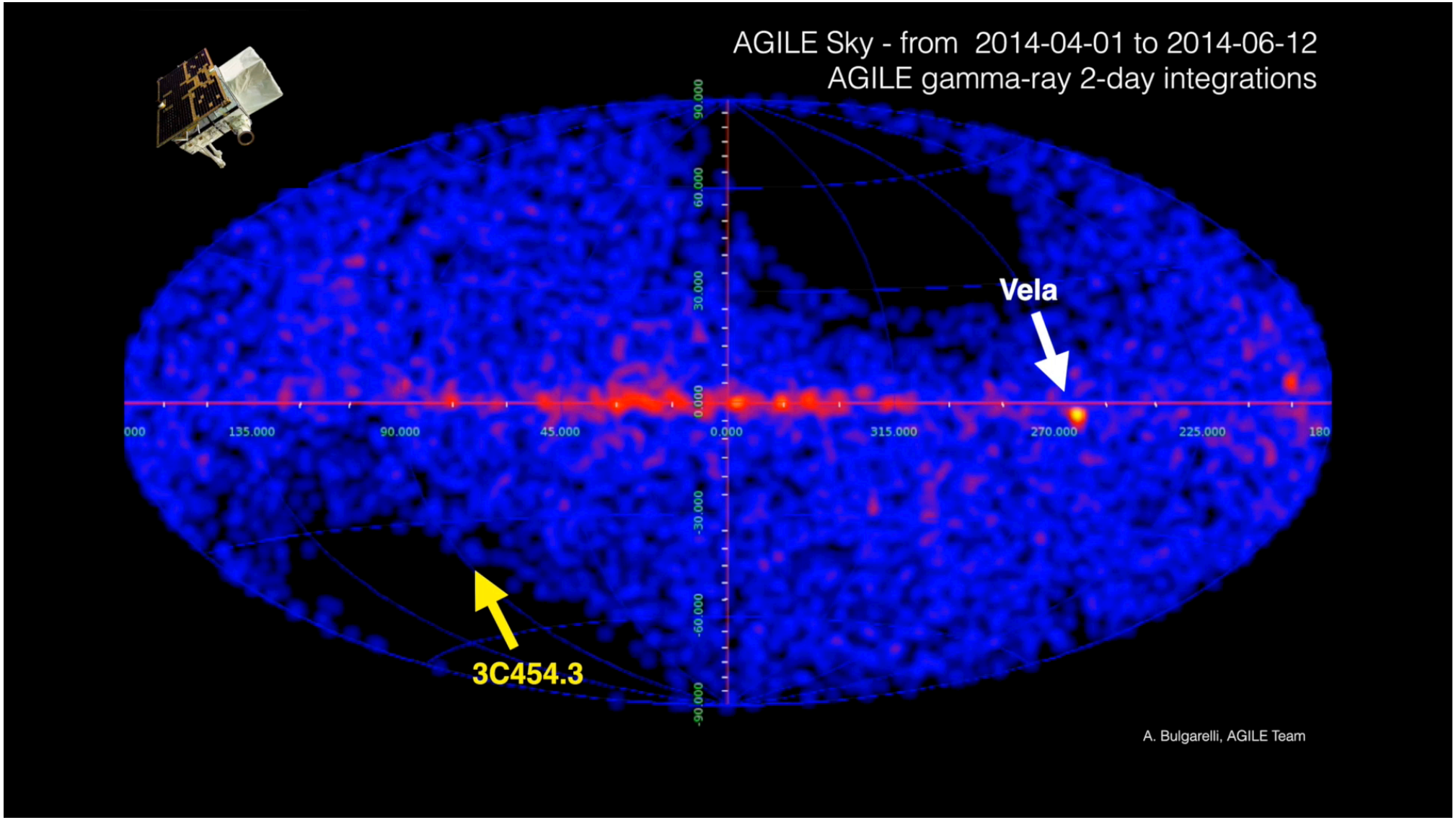
AGILE Sky - from 2014-04-01 to 2014-06-12
AGILE gamma-ray 2-day integrations
Vela
3C454.3
A. Bulgarelli, AGILE Team
90.000
60.000
30.000
0.000
-30.000
-60.000
-90.000
135.000
90.000
45.000
0.000
315.000
270.000
225.000

FERMI

Andrea Bulgarelli (bulgarelli@iasfbo.inaf.it)

Fermi, NASA

The Fermi Observatory

Large AreaTelescope (LAT)
20 MeV - >300 GeV

Gamma-ray Burst Monitor (GBM)
NaI and BGO Detectors
8 keV - 40 MeV

KEY FEATURES

- **Field of view**
  - **– LAT: 2.4 sr; 20% of the sky at any instant (the same of AGILE);**
  - **– GBM: whole unocculted sky at any time.**
- **Every photon can be time-tagged.**
  - **– 1 microsecond accuracy**

Launched June 11, 2008

Fermi – LAT

from G. Kanbach

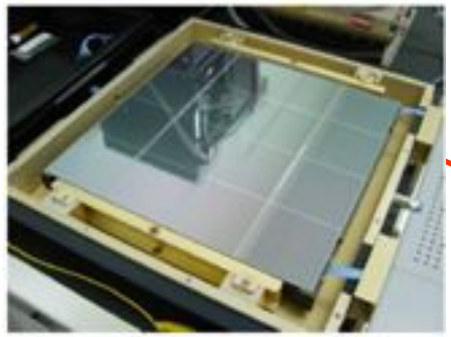

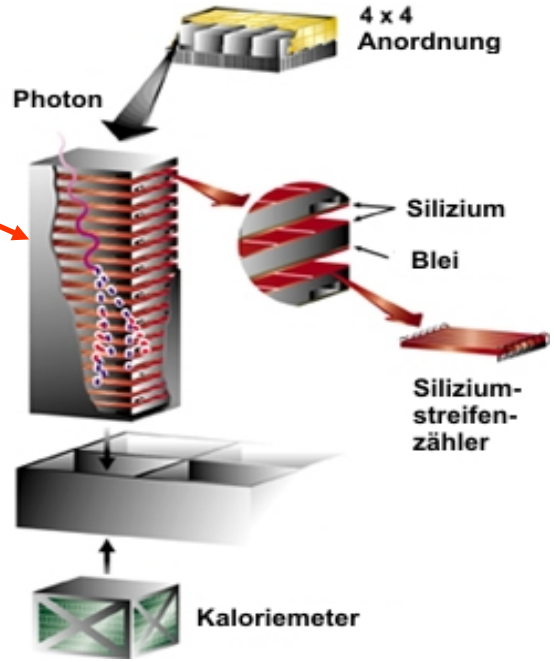

The 18 tungsten converter layers and 16 dual silicon tracker planes are stacked in 16 modular "towers" (37 cm square and 66 cm tall). Each of the 16 calorimeter modules consists of 96 long, narrow CsI scintillators, stacked in 8 layers, alternating in orientation so that the location and spread of the deposited energy can be determined. The plastic anticoincidence scintillator around the outside is made of 89 individual sections so that it can distinguish charged particles coming from the direction of the incident gamma ray and ignore others.

The LAT is 0.72 m deep and 1.8 m square. Its total mass is **2789 kg**. It uses 650 W of electric power.

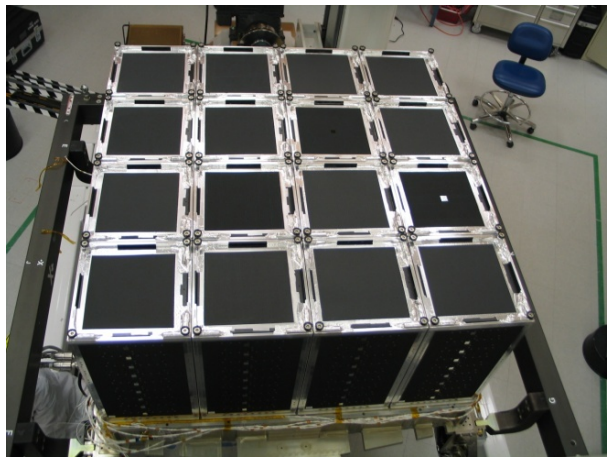

… a tracker of stacked Si strip detectors

Fermi/NASA

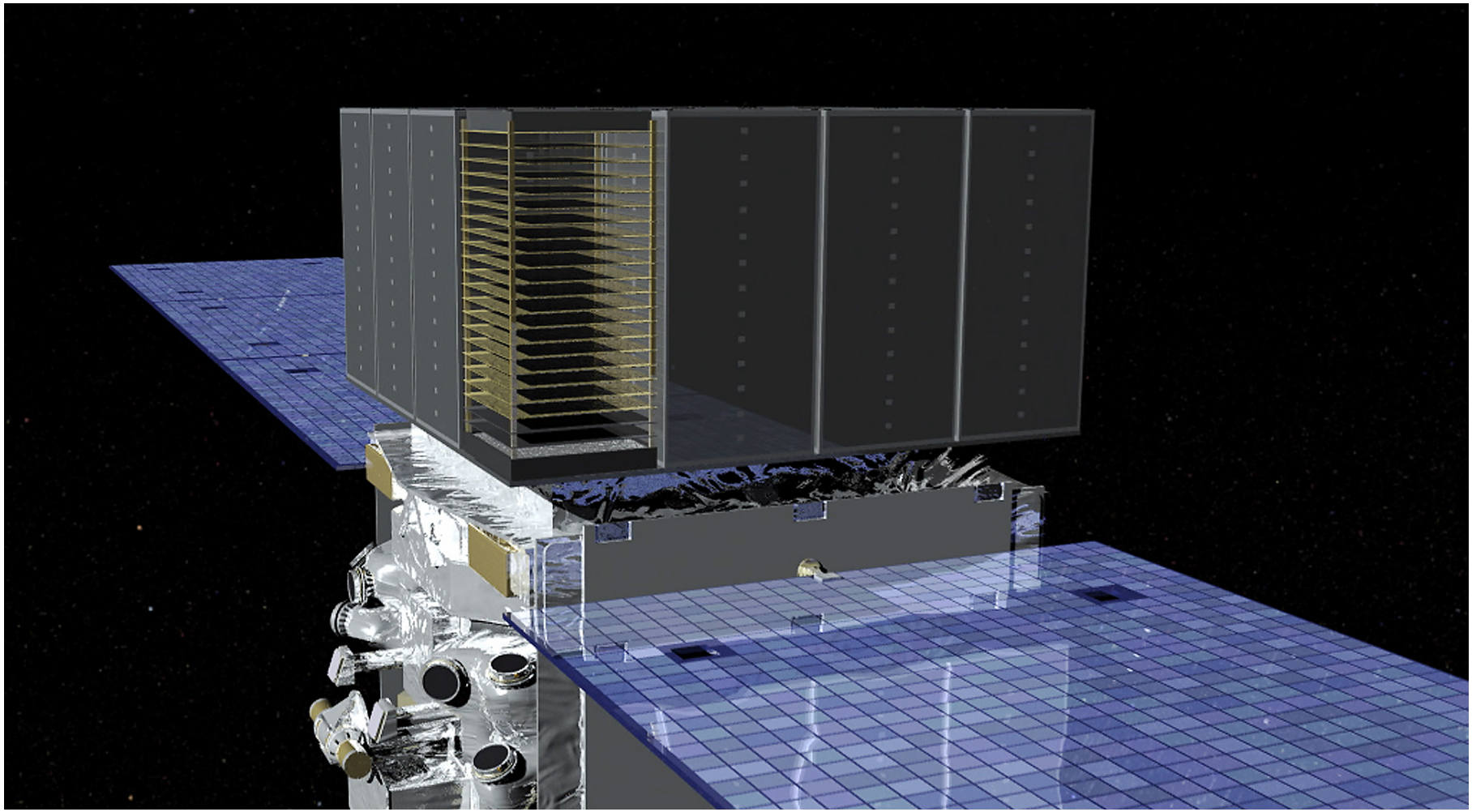

Andrea Bulgarelli (bulgarelli@iasfbo.inaf.it)

CTA

Andrea Bulgarelli (bulgarelli@iasfbo.inaf.it)

CTA – A NEW WINDOW ONTO THE VIOLENT UNIVERSE

cta
cherenkov telescope array

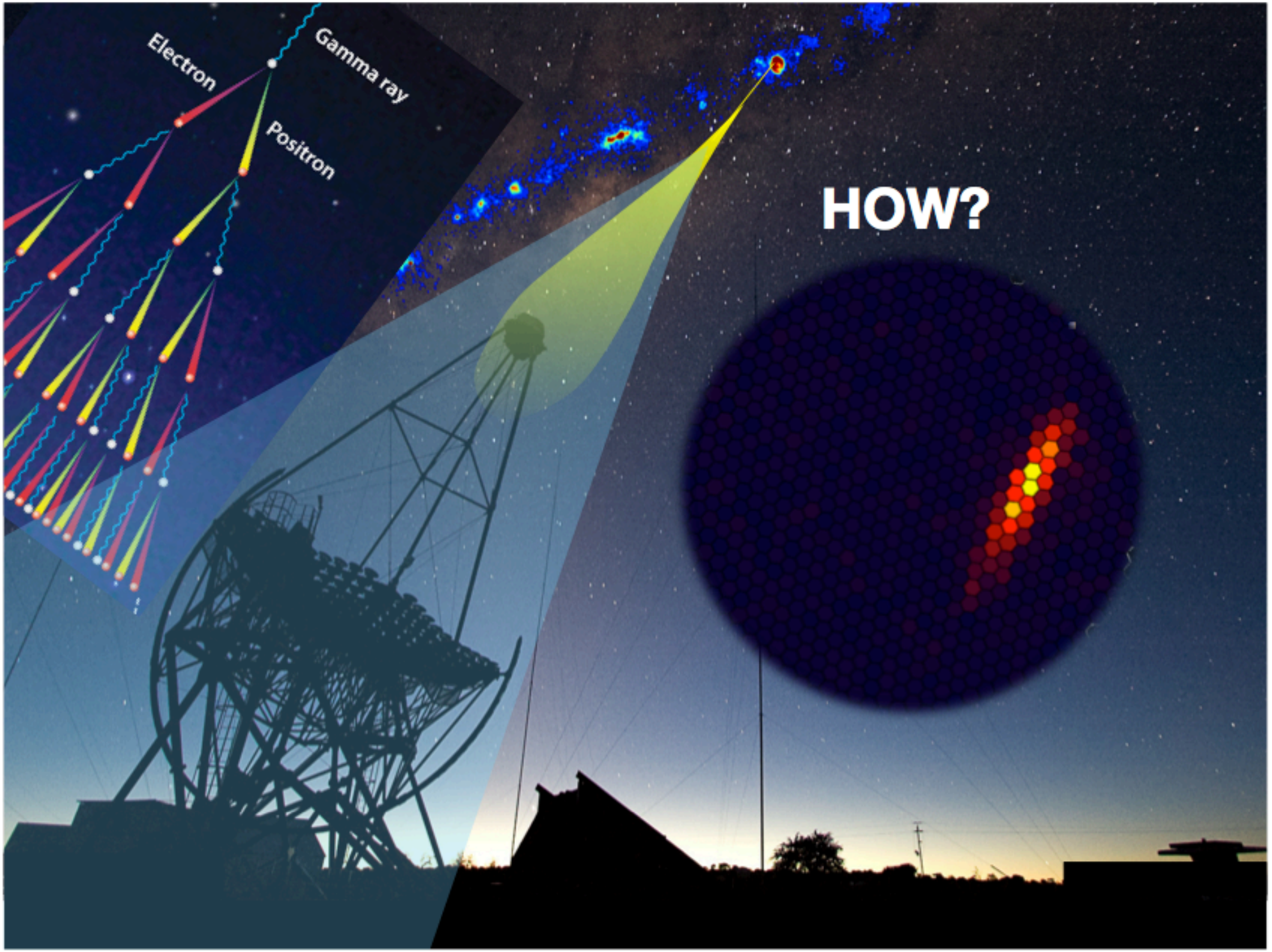
Electron
Gamma ray
Positron
HOW?

CURRENT IACT EXPERIMENTS

FACT, La Palma
1 x 9.5 m^2 telescopes

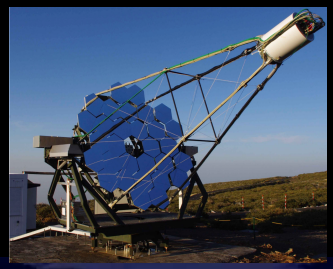

FACT

MAGIC Canary Islands 2200 m asl
2 x 17m telescopes. Magic I in operation since Oct 2003, Magic II first light shown at ICRC09

VERITAS Arizona, USA 1800 m asl
4 telescopes of 12m diameter
fully operational from fall 2007

MAGIC

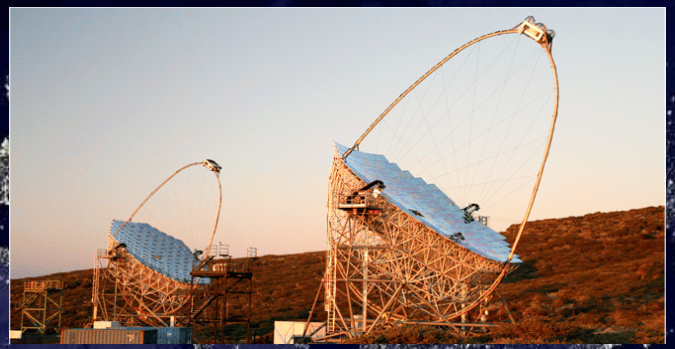

MAGIC

VERITAS

VERITAS

HESS Namibia 1800 m asl
HESS I: 4 telescopes of 12m diameter
HESS II: 28 m diameter

HESS

HESS

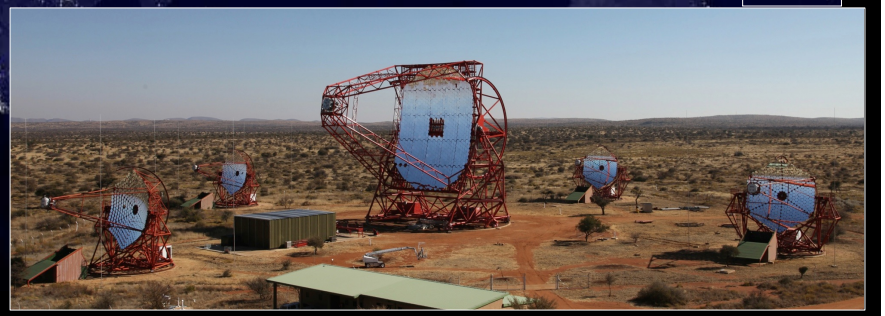

Dec 2003: 4 telescope commissioned
2014: HESS II commissioning

CTA SITES

One Observatory with two (asymmetric) sites for all-sky coverage

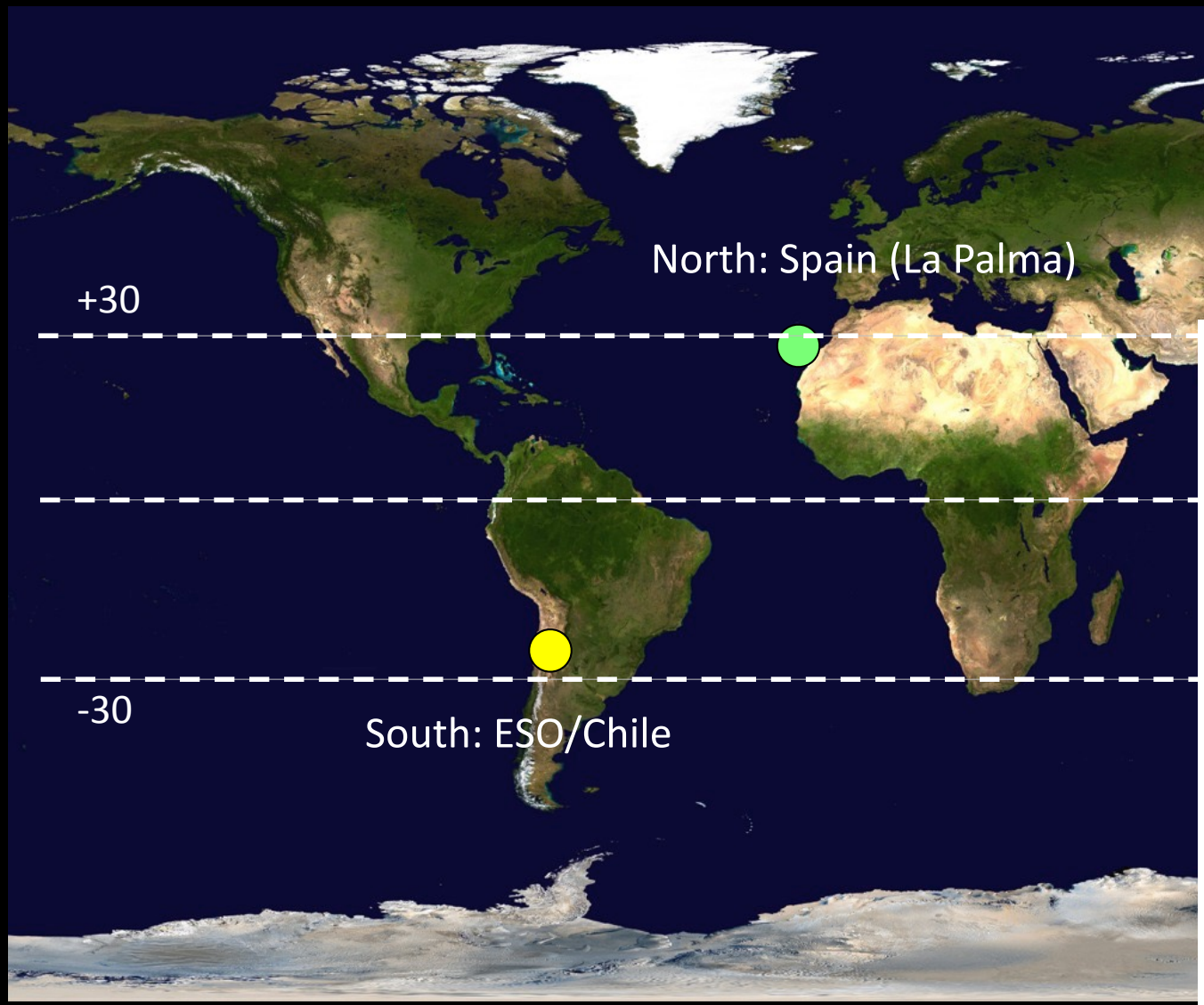

Northern Array

- complementary to SA for full sky coverage
- Energy range: some 10 GeV to few TeV
- Limited field of view

Mainly Extragalactic Sources

Southern Array

- Full energy and sensitivity coverage: some 10 GeV to above 100 TeV
- Angular resolution: 0.02 to 0.2 deg
- Large field of view

Galactic + Extragal. Sources

X

IACT = IMAGING AIR CHERENKOV TELESCOPES

UV-optical reflecting mirrors focussing flashes of Cherenkov light produced by air-showers into ns-sensitive cameras.

"Shower"

For E=1 TeV ($E_C \approx 80$ MeV)

$X_{max} \cong X_0 \ln(E/E_C) / \ln 2$

$h_{max} = h_0 \ln(X_A/X_{max}) \rightarrow 5$ km

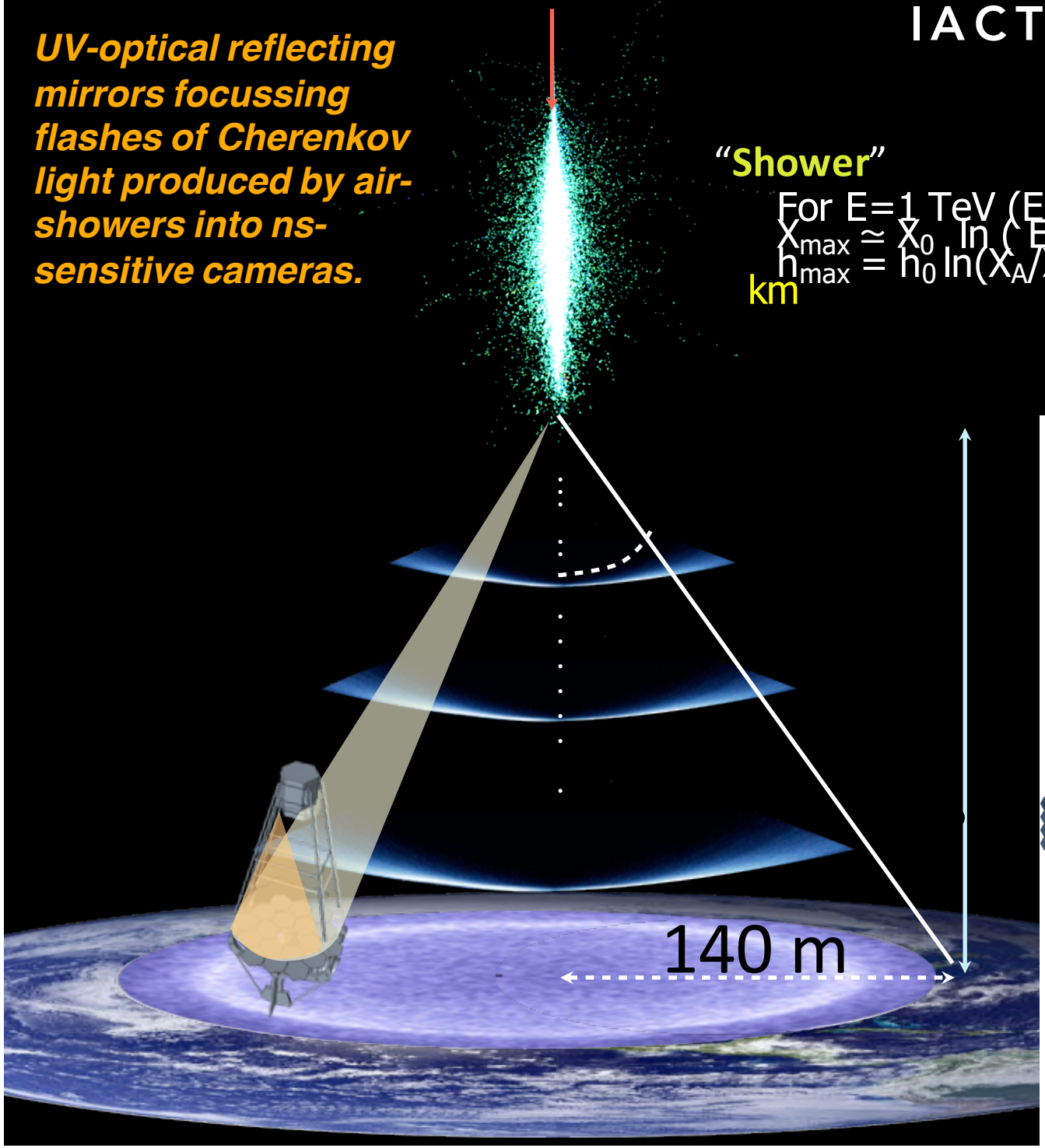

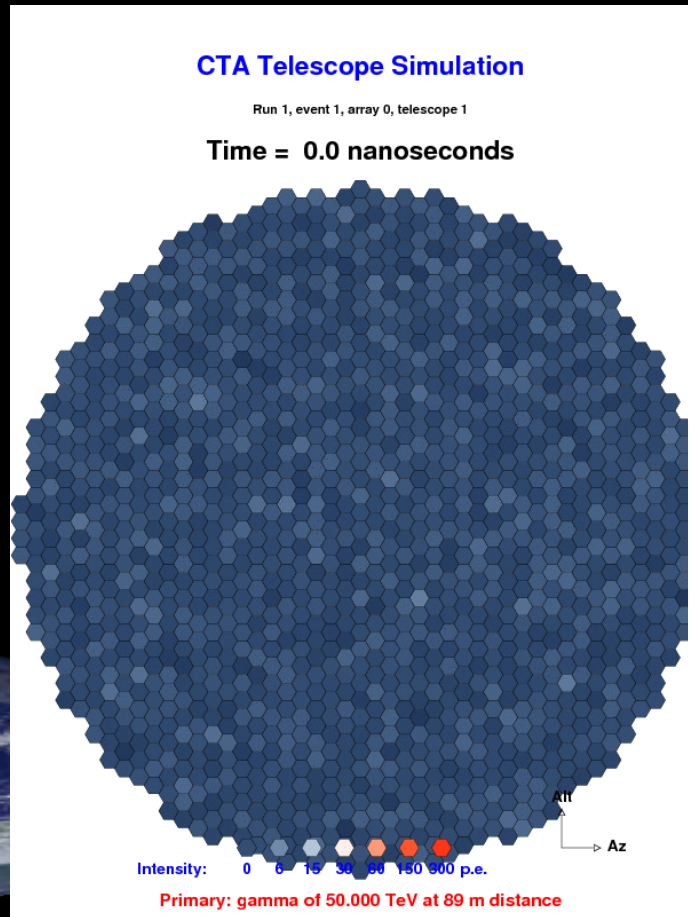

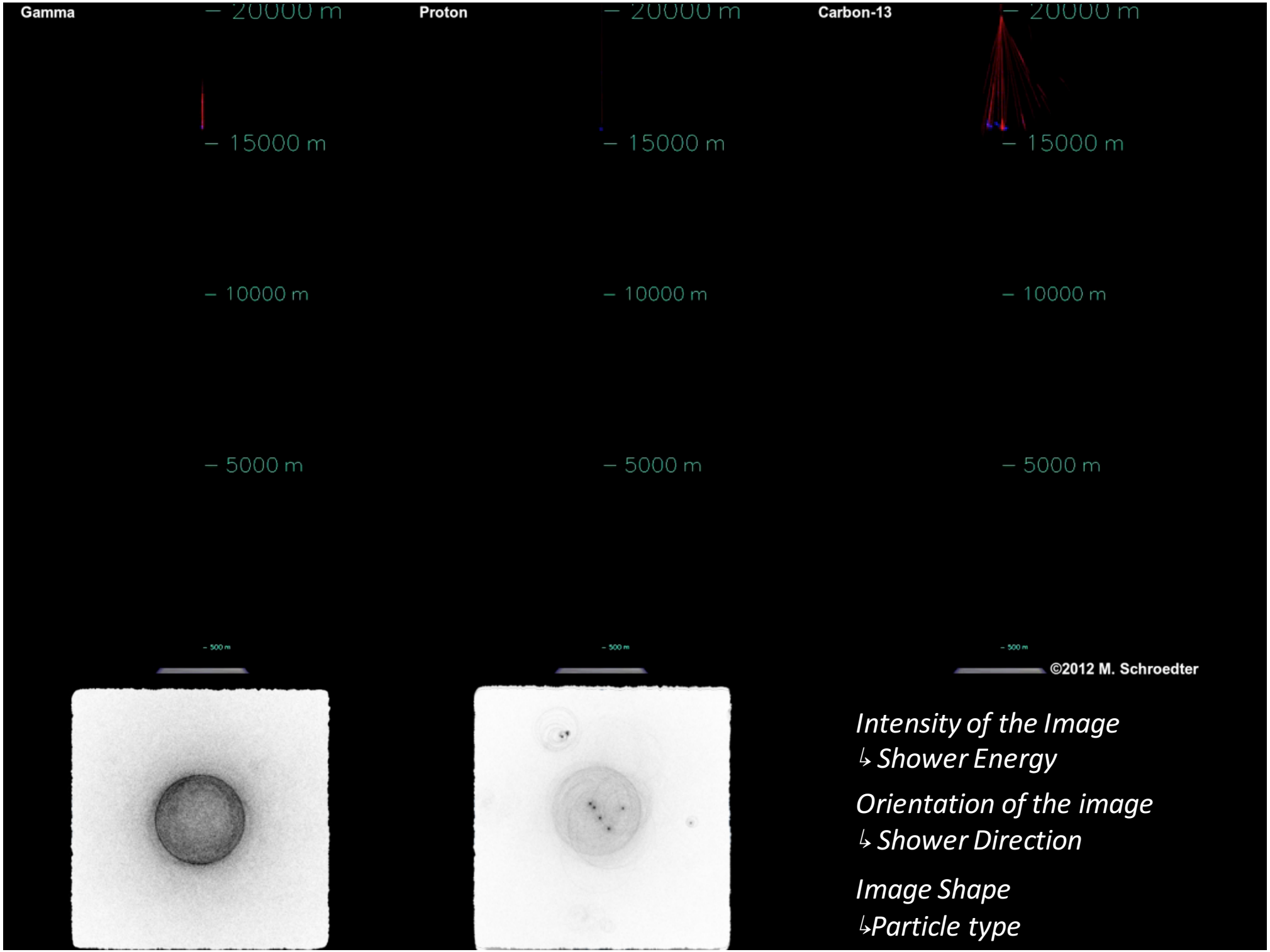
Gamma
Proton
Carbon-13
– 20000 m
– 15000 m
– 10000 m
– 5000 m
– 500 m
©2012 M. Schroedter
Intensity of the Image
↳ Shower Energy
Orientation of the image
↳ Shower Direction
Image Shape
↳Particle type

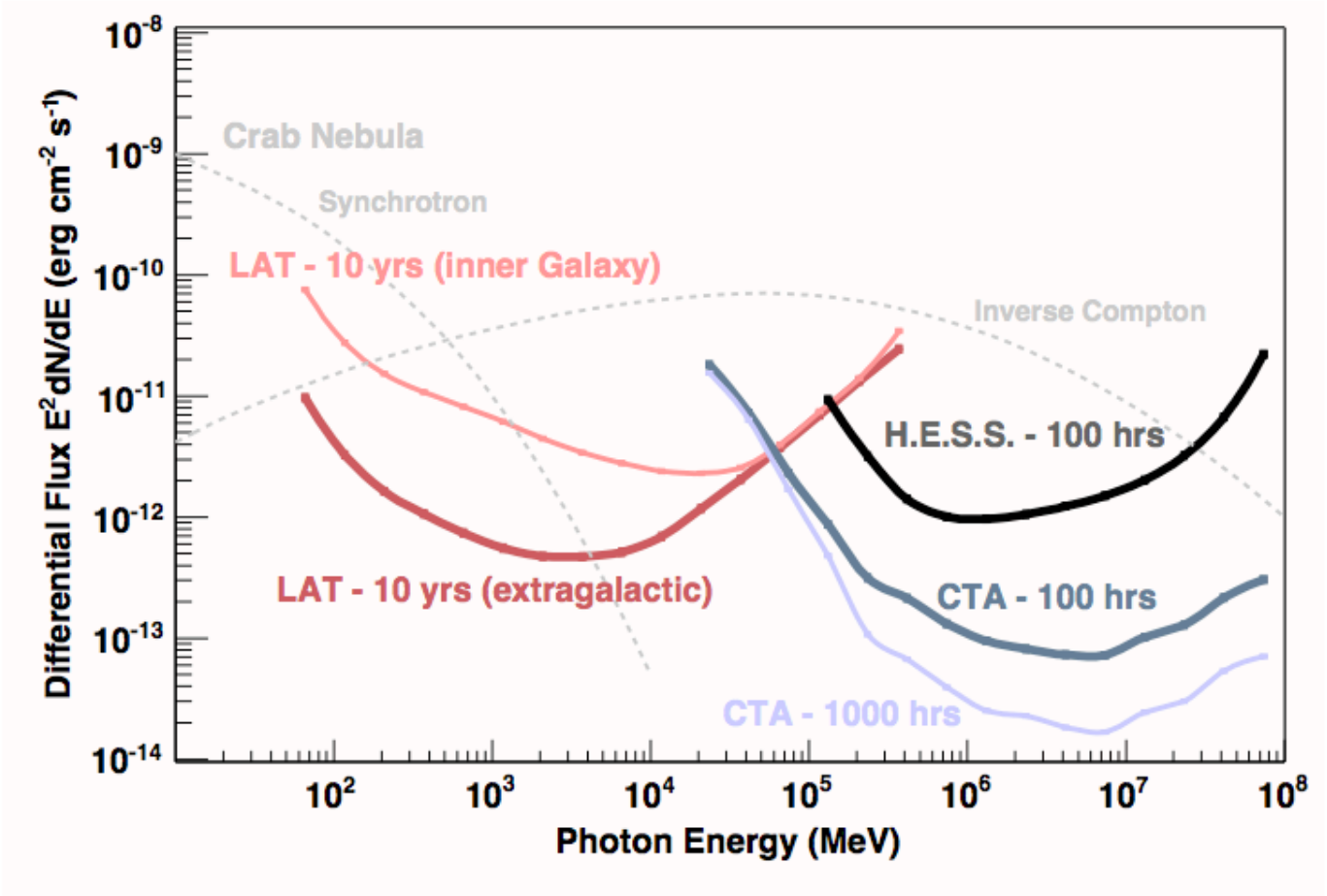

Figure 1: "Differential" sensitivity (integral sensitivity in small energy bins) for a minimum significance of 5σ in each bin, minimum 10 events per bin and 4 bins per decade in energy. For Fermi-LAT, the curve labeled "inner Galaxy" corresponds to the background estimated at a position of $l = 10°, b = 0°$, while the curve labeled "extragalactic" is calculated using the isotropic extragalactic diffuse emission only. For the ground-based instruments a 5% systematic error on the background estimate has been assumed. All curves have been derived using the sensitivity model described in section 2. For the Fermi-LAT, the *pass6v3* instrument response function curves have been used. As comparison, the synchrotron and Inverse Compton measurements for the brightest persistent TeV source, the Crab Nebula are shown as dashed grey curves.

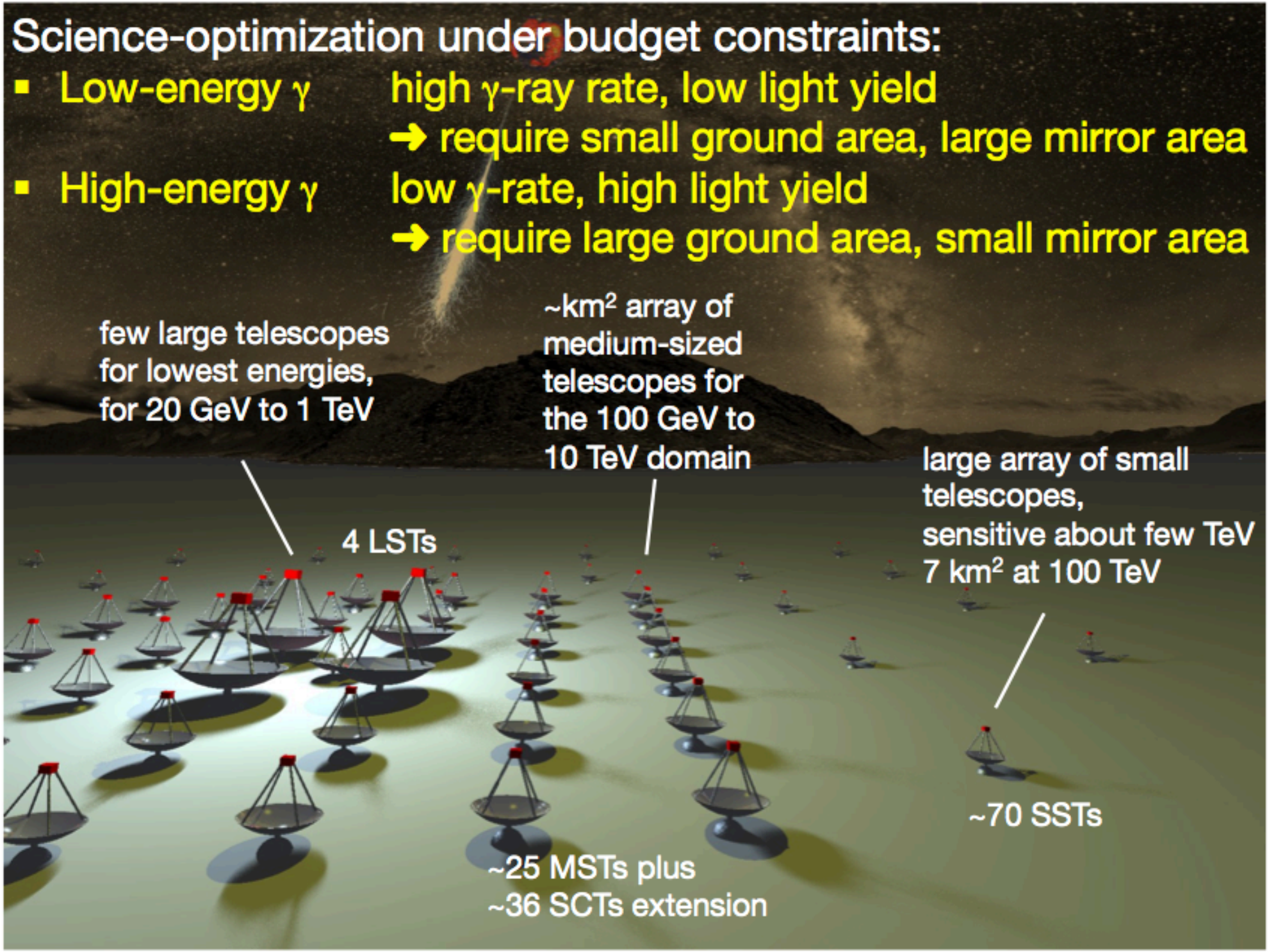
Science-optimization under budget constraints:
Low-energy γ high γ-ray rate, low light yield
➜ require small ground area, large mirror area
High-energy γ low γ-rate, high light yield
➜ require large ground area, small mirror area
few large telescopes for lowest energies, for 20 GeV to 1 TeV
~km² array of medium-sized telescopes for the 100 GeV to 10 TeV domain
large array of small telescopes, sensitive about few TeV 7 km² at 100 TeV
4 LSTs
~25 MSTs plus ~36 SCTs extension
~70 SSTs

References

- Giacconi, R., et al. 1968, *Observational Techniques in X-Ray Astronomy*, Annual Review of Astronomy and Astrophysics, 6, p. 373
- Gursky, H., & Schwartz, D. 1974, in *X-Ray Astronomy*, R. Giacconi & H. Gursky eds., (Boston: D. Reidel), Chapter 2, pp. 44–52
- Peterson, L.E. 1975, *Instrumental techniques in X-ray astronomy*, Annual Review of Astronomy and Astrophysics, 13, p. 423
- Zombeck, M.V., 1990, *Handbook of Space Astronomy & Astrophysics*, 2nd ed., Cambridge University Press
- Fraser, G.W., 1989, *X-ray Detectors in Astronomy*, Cambridge University Press, 1989
- Knoll,G.F., 2000, *Radiation Detection and Measurement*, 3rd ed., John Wiley 2000
- http://xmm.esac.esa.int/external/xmm_user_support/documentation/technical/
- http://cxc.harvard.edu/proposer/POG/html/index.html
- http://space.mit.edu/~jonathan/xray_detect.html
- http://physics.nist.gov/PhysRefData/XrayTrans/Html/search.html

Attività principali del nostro gruppo:

- Simulazioni Monte Carlo di telescopi X e Gamma per la minimizzazione del fondo
- Sviluppo di telescopi futuri X e Gamma
- Sviluppo di software di analisi dati (ad esempio allerte in tempo reale dallo spazio)
- Analisi dati e data mining
  - Ricerca della controparte elettromagnetica delle onde gravitazionali
  - Sviluppo di nuovi algoritmi di analisi di transienti gamma

Il telescopio ATHENA (Advanced Telescope for High-ENergy Astrophysics):

- Telescopio X approvato dall'Agenzia Spaziale Europea
- Lancio nel 2028
- Tante le sfide:
  - Nuova tecnologia per le ottiche X
  - Per la prima volta microcalorimetro X ad altissima risoluzione energetica
  - Orbita in L2
  - Minimizzazione del fondo cruciale

Raggi gamma dallo spazio:

- AGILE: Telescopio gamma in volo dal 2007
  - Ora parte dell'LIGO-EM MoU:
    - Analisi veloce di transienti gamma
    - Ricerca di controparte EM di onde gravitazionali
- ASTROGAM: proposta sottomessa a M5. Lancio previsto 2028

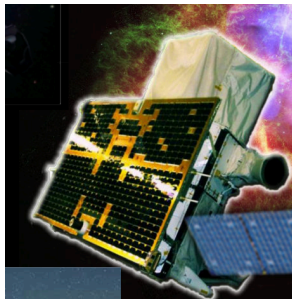

Raggi gamma da terra:

- CTA: real-time analysis

Volete saperne di più?
Scriveteci!